FACULTY OF ELECTRICAL ENGINEERING

MODELLING AND ANALYSIS OF SENSORLESS PERMANENT MAGNET SYNCHRONOUS MOTOR BY USING FUNDAMENTAL EXCITATION

Siti Zahrah binti Anuar

Bachelor of Electrical Engineering

2016

APPROVAL FORM

" I hereby declare that I have read through this report entitle "Modelling and Analysis of Sensorless Permanent Magnet Synchronous Motor by using Fundamental Excitation" and found that it has comply the partial fulfilment for awarding the degree of Bachelor of Electrical Engineering (Industrial Power)"

Signature : .....

Supervisor's Name : DR. JURIFA BINTI MAT LAZI

Date : .....

MODELLING AND ANALYSIS OF SENSORLESS PERMANENT MAGNET SYNCHRONOUS MOTOR BY USING FUNDAMENTAL EXCITATION

SITI ZAHRAH BINTI ANUAR

A report submitted in partial fulfilment of the requirements for the degree of Bachelor of Electrical Engineering (Industrial Power)

Faculty of Electrical Engineering

UNIVERSITI TEKNIKAL MALAYSIA MELAKA

2016

I declare that this report entitle “Modelling and Analysis of Sensorless Permanent Magnet Synchronous Motor by using Fundamental Excitation” is the result of my own research except as cited in the reference. The report has not been accepted for any degree and is not concurrently submitted in candidature of any other degree.

Signature : .....

Name : SITI ZAHRAH BINTI ANUAR

Date : .....

To my beloved mother and father

ACKNOWLEDGEMENT

First and foremost, I would like to express my thanks to Allah for giving me strength and ability to complete this final year project in time. I would like to express my great appreciation to my supervisor Dr Jurifa Binti Mat Lazi for her guidance and advice that really help me to understand about my topic.

Next, I would also like to thanks my friends who have shared some knowledge in completing this report. Last but not least, a special thanks to my parents that always gives their morale support and motivation throughout the entire process of completing this report.

ABSTRACT

Over the past few years, the usage of sensorless motor drive has been widely used in various servo applications for its reliability, lower cost and small size. The most common type of motor drive used is Permanent Magnet Synchronous Motor (PMSM). This project presents the sensorless PMSM by using fundamental excitation. Permanent Magnet Synchronous Motor is used because during transformation of abc to direct and quadrature (d-q), the sinusoidal varying inductance will become constant in d-q frame. In which show that PMSM is suitable to be used in d-q system. However the operation of PMSM requires sensor to determine the rotor position. The problem about sensor is the high cost, machine size and it will decrease the reliability of the system. Besides that, research being done about sensorless PMSM experimentally is less compared to motor drive with sensor. Therefore sensorless method is presented to overcome the problems mentioned. Sensorless motor drives uses complex Clarke's and Park's transform to determine the shaft positions, thus making it more reasonable to be used with the PMSM. The aim of this study is to model, develop, simulate and investigate the behavior of sensorless Permanent Magnet Synchronous Motor drives using Fundamental Excitation. The results prove that the speed and position estimator is capable to give output response near to the actual speed.

ABSTRAK

Sejak beberapa tahun kebelakangan ini, penggunaan pemacu motor tanpa sensor telah digunakan secara meluas dalam pelbagai aplikasi servo kerana faktor seperti kebolehpercayaan, kos yang lebih rendah dan saiz kecil. Jenis pemacu motor yang paling banyak digunakan ialah magnet kekal motor segerak. Projek ini membentangkan tentang sistem magnet kekal motor segerak tanpa sensor dengan menggunakan pengujaan asas. Magnet kekal motor segerak digunakan kerana semasa transformasi abc ke mengarah dan kuadratur (d-q), kearuhan mengubah sinusoidal akan menjadi tetap di dalam bingkai d-q. Ini, menunjukkan bahawa magnet kekal motor segerak adalah sesuai untuk digunakan dalam sistem d-q. Untuk magnet kekal motor segerak beroperasi, ianya memerlukan sensor untuk menentukan kedudukan pemutar. Walaubagaimanapun, pengunaan sensor mempunyai beberapa kelemahan seperti kos yang tinggi, saiz mesin dan turun kebolehpercayaan sistem. Selain daripada itu, kajian yang dilakukan mengenai magnet kekal motor segerak tanpa sensor adalah kurang berbanding dengan sistem yang menggunakan sensor. Pemacu motor tanpa sensor menggunakan kaedah penukaran Clarke dan Park untuk menentukan kedudukan aci, menjadikan ia lebih sesuai untuk digunakan dengan magnet kekal motor segerak. Tujuan kajian ini dijalankan adalah untuk mereka bentuk, membangunkan , simulasi dan menyiasat kelakuan pemacu motor tanpa sensor menggunakan pengujaan asas. Berdasarkan keputusan simulasi, ianya membuktikan bahawa kelajuan dan kedudukan penganggar mampu untuk memberikan keluaran tindak balas berhampiran dengan kelajuan sebenar.

TABLE OF CONTENTS

LIST OF TABLE

LIST OF FIGURES

LIST OF ABBREVIATIONS

PMSM	-	Permanent Magnet Synchronous Motor
IM	-	Induction Motor
PM	-	Permanent Magnet
SVPWM	-	Space Vector Pulse Width Modulation
d-q	-	Direct and Quadrature
BDCM	-	Brushless DC Motor
EKF	-	Extended Kalman Filter
DSP	-	Digital Signal Processor
FPGA	-	Field Programmable Gate Array
FSM	-	Finite State Machine
BEMF	-	Back Electromotive Force
AC	-	Alternating Current

CHAPTER 1

INTRODUCTION

1.1 Overview

In recent years, Induction Motor (IM) and PMSM are becoming popular among machine drives. Permanent Magnet (PM) motor drives have been receiving much attention due to its significant advantages capability to operate at high motor and high energy efficiency with wide speed ranges. A PMSM is an AC synchronous motor that uses permanent magnet rather than windings in the rotor to produce air gap magnetic field rather than using electromagnetic. The PMSM is extensively used in the industry for several different reasons such as its high torque to inertia ratio and superior power density compared to other motors. Other advantages of PMSM include compactness, high performance motion control with fast speed and better accuracy.

1.2 Motivation

The design of PMSM does not require commutator equipped with brushes as there is no need to supply current to the rotor. This is because it uses permanent magnet rather than winding in the motor. Input of a PMSM can be analogue voltage or switches. The switches can be controlled using two methods which are SVPWM and Hysteresis current controller. In this project the control scheme used is SVPWM as it has high magnitude of

output voltage. Simulation of the permanent magnet motor drive system of this project is developed by using MATLAB/Simulink.

In allowing effective vector control of a permanent magnet synchronous motor, a motor shaft position sensor is needed. The sensor is placed in rotor shaft in order to operate a PMSM. However the sensor increases the cost of the drive and reduces its reliability. Other than that, PMSM is known to be constructed with fixed rotor field which is supplied by rotor mounted magnet. The rotor position can be obtained by using resolver and encoder but then the components used contributed several disadvantages such as noise immunity and reliability. By taking into consideration the disadvantages mentioned, a sensorless control of permanent magnet synchronous motor is suggested to be used. The sensorless technologies are able to increase the reliability and reduce the cost. A benefit of the sensorless control is it can be use in small space because it replaces encoder or resolver with estimator.

1.3 Project Background

1.3.1 Permanent Magnet Synchronous Motor Drive System

A motor drive system consists of four main components which include Permanent Magnet motor, inverter, control unit and position sensor. The motor drive system is as shown below in Figure 1.1.

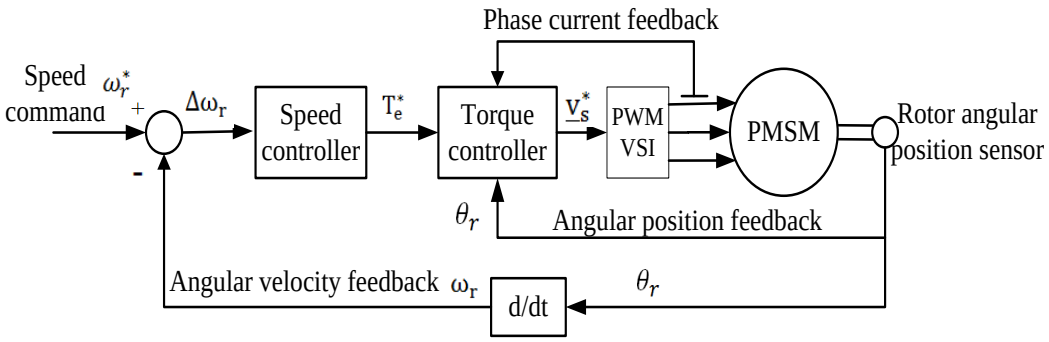

Figure 1.1: Motor drive system [10]

1.3.2 Permanent Magnet Synchronous Motor

A PMSM is an AC synchronous motor that uses permanent magnet rotor to produce the air gap magnetic field. PMSM motor is attracting industry sector and researchers to use it in varies of application because it can perform at high torque and low speed, good energy density and have higher energy efficiency than other motors.

I. Permanent magnet radial field motors

In PM motor, there are two different configurations on how the magnet can be placed in the rotor [10]. The two types of magnet configurations are surface permanent magnet motor or interior permanent magnet motor [11].

Surface PM motor magnet position is mounted in the surface of the rotor. It is simple to build as the PM is mounted on the surface of the rotor. Furthermore to reduce cogging torque, specially skewed poles that are easily magnetized are placed on this surface mounted type. This kind of structure is used for low speed application as magnets will fly apart in high speed operation. Since these motor have small saliency, it have equal inductance for both axes. The relative permeability of permanent magnet is close to one which cause machine to have large effective air gap. Surface permanent magnet is a nonsalient pole so, that the direct axis's inductance and quadrature axis's inductance are same ($L_d = L_q$) [12]. The rotor has an iron core that may be solid or may be made of punched laminations for simplicity in manufacturing [10]. Adhesives are used to mount the thin permanent magnet on the surface of its core. Radial directed flux density across the air gap is produce by the alternating process of magnet of the opposite magnetization direction. In producing torque the produced flux density then react with the current in windings located in slots of the inner surface of stator. Figure 1.2 below shows the motor cross section.

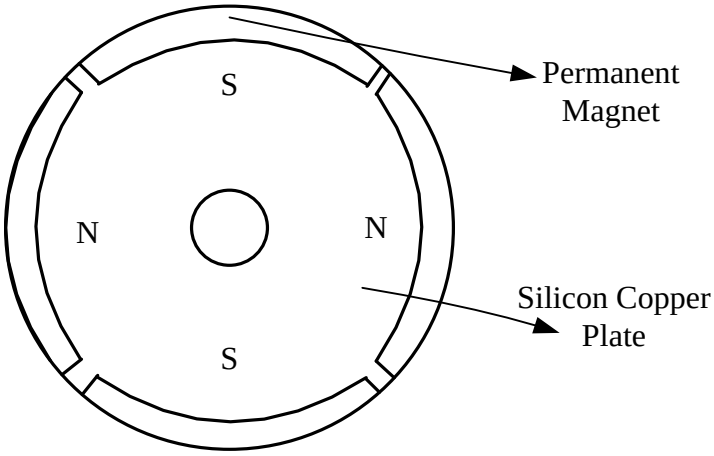

Figure 1.2: Surface Permanent Magnet motor [12]

Unlike surface permanent magnet motor, the interior permanent magnet motor magnets are mounted inside the rotor. The most typical configuration is shown Figure 1.3. The difference geometrical shape of the magnet compared to the normal shape allows a much higher speed operation. Since the air gap of direct axis is larger than quadrature axis, the machine is considered having salient pole ($L_d < L_q$) [12].

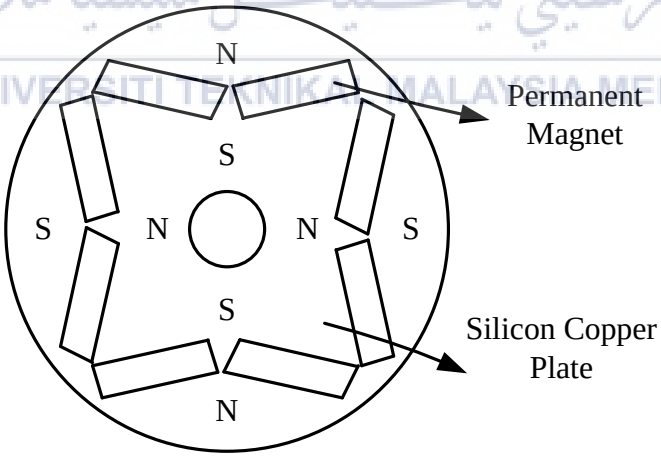

Figure 1.3: Interior Permanent Magnet motor [12]

1.3.3 Position Sensor

Position sensor is placed in rotor shaft to operate a PMSM. In order for the rotor position to be known, position measurement device can be use. A few of the devices used to measure the position includes optical encoder, linear variable differential transformer, potentiometer and resolver. Among them, the most commonly used for motors are resolver and encoders. However the price of a position sensor is expensive and a special mechanical arrangement needs to be made for mounting the position sensors and extra signal wires are required to be attached from the sensor to the controller.

i. Optical Encoders

Optical encoder design consists of LED light source, light detector, rotating disk and light sensor (photo detector). The disk has opaque and transparent segment and is placed at the shaft. As it rotate, the disc intercept light beams to create codded pattern or generate digital pulse. The optical encoder is as shown in Figure 1.4. There are two types of encoder which are incremental encoder and absolute encoder

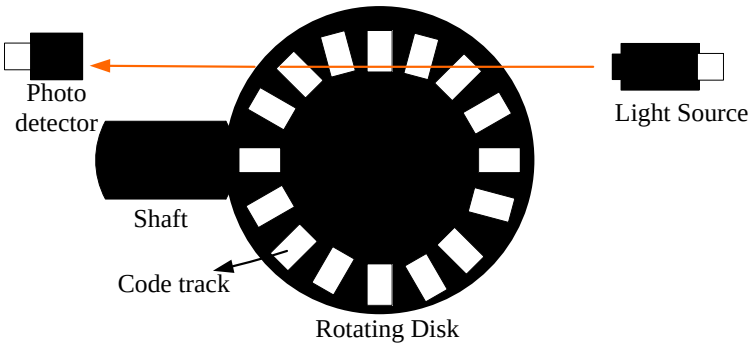

Figure 1.4: Optical Encoder [13]

i. Incremental encoders

Incremental encoders consist of two squares waves as their output with each corresponding to increase of rotation. The output from the encoder consists of two detection signal known as “A” and “B” to detect position. The beam is split to produce a beam light 90° degrees out of phase. The light “A” and “B” passes through the disc and is then converted into two square signal, widely known as quadrature output indicating the position and direction of rotation. If “B” leads “A”, the disk rotates in a counter clockwise direction and vice versa if “A” leads “B”. Incremental encoders also include a third output channel called as zero that supplies a single pulse per revolution. This third signal is used to acquire precise reference position. Figure 1.5 shows the channels of quadrature encoder.

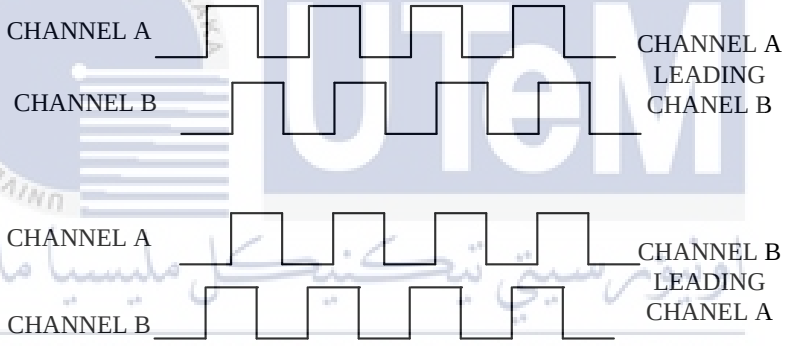

Figure 1.5: The channels of quadrature encoder for an Incremental encoder [28].

ii. Absolute encoders

Each position of absolute condition is provided by a binary “word”. Absolute means that every position is unique. The combination of numbers of channel determines how high resolution is possible. In determining the actual position, the encoder will emit a combination of signals with precision directly related to the number of bits in the encoder. Absolute encoder does not need to find fixed reference point. This is because it can still

measure or obtain the exact position as soon as the voltage is turned on and even if the motor stop.

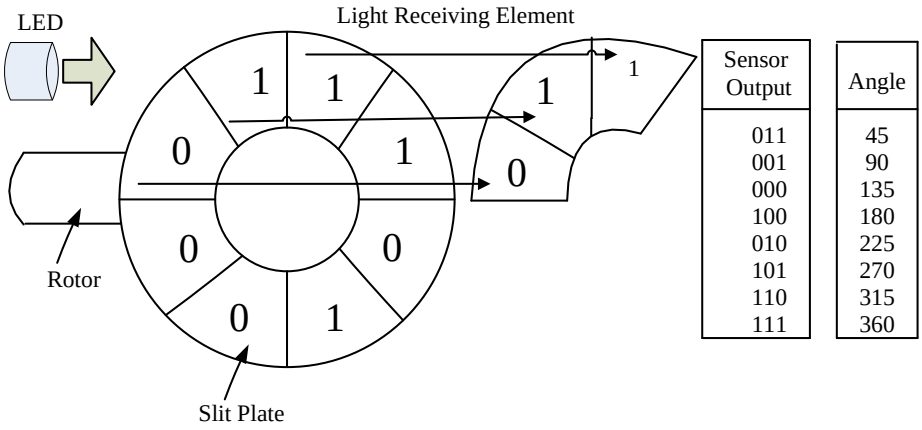

Figure 1.6: Absolute encoder [28]

The output from these detectors is depending on the code disc pattern for that particular position either HI (light) or LOW (dark). Absolute encoders are mainly used in robotic tools in which the device is usually moves at a slow rate [14]. The absolute encoder is shown in Figure 1.6 above.

1.3.4 Position Revolver

Position revolver operates on the principle of transformer. It is also called as rotary transformers as shown in Figure 1.7. To obtain the position of motor, the primary winding is mounted on the rotor and the secondary windings are wound at 90° to each other on the stator core [15]. Position using revolver can be obtained using the two voltages. In simple word a resolver control transmitter consists of one rotating reference winding (V_{ref}) and two secondary winding (V_{sin} , V_{cos}). The reference winding is located in the rotor while the secondary winding is located at the stator. The two stator winding are placed 90° from one another thus generating the cos and sine voltages. Hence onward the two stator winding is

referred as output windings. The voltage induced into the rotor is proportional with angular movement of the motor shaft (θ).

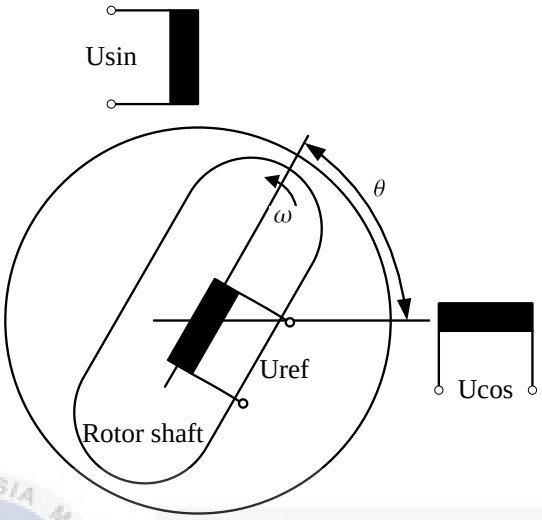

Figure 1.7: Structure of resolver [28]

The generated voltage frequency is similar to the reference voltage. Changes to the sine and cosine of the shaft angle vary their amplitude. If one of the output windings is aligned with the reference winding, thus full voltage is generated on that output and on the other output is zero voltage and vice versa [16]. Other than that, the rotor angle (θ_r) can be obtained from the voltage. Using the resolver output voltage (V_{sin} and V_{cos}) the shaft angle can be determined by an Inverse tangent [12] relationship expressed as in equation (1.1)

$$\theta = \alpha \, tan(\frac{U \, sin}{U \, cos}) \tag{1.1}$$

1.4 Problem Statement

Recently, motor drive systems are widely used in various servo applications. The most used motor drive is PMSM as it has high-performance motion control with fast speed and accuracy. PMSM have permanent magnet located at the rotor, back electromotive force (EMF) and need stator current in producing constant torque [8]. PMSM uses permanent magnet to generate excitation and it does not have damper winding. Therefore it is suitable to be use in the direct and quadrature (d-q) model. In transforming three phase abc model to d-q, it causes the sinusoidal varying inductance to become constant in d-q frame [9]. However a major drawback to allow effective vector control of a PMSM is the position sensor. The usage of the position or speed sensor implies more space, extra wiring, additional electronic, frequent maintenance, high price, noise immunity, drive cost and decrease in reliability. In need to avoid these disadvantages a sensorless drives is used. The elimination of the sensor that is used to measure and calculate the shaft speed and position will reduce hardware complexity, size and allow cable elimination. Other advantages of the sensorless motor drives include the increase in reliability, increase in noise immunity, less maintenance and it lower the cost of the drive. There are several sensorless methods such as adaptive observer, sliding mode observer (SMO) and EKF. However by comparing the advantages and disadvantage for each sensorless technique, the speed and position estimator using adaptive controller is selected as its uses simple equation and system structure.

Besides that lack numbers of research is being done in sensorless PMSM drive compared to PMSM drive with sensor. Most of the analysis that has been done, only study about the simulation. In addition, some of the position sensors are temperature sensitive and their accuracy deteriorates when the system temperature exceeds the limit [10]. Therefore a sensorless method is introduced to replace the position sensor.

1.5 Objectives

The objectives of this project are:

1. To model and develop sensorless Permanent Magnet Synchronous Motor (PMSM) drives using Fundamental Excitation.
2. To simulate the sensorless Permanent Magnet Synchronous Motor (PMSM) drives using Fundamental Excitation
3. To investigate the behaviour of sensorless Permanent Magnet Synchronous Motor (PMSM) drives for wide speed range and load variation

1.6 Scope

The scope of this project is to conduct simulation study of PMSM drives using fundamental excitation. The MATLAB/Simulink software is used to simulate and analysed the behaviour of sensorless Permanent Magnet Synchronous Motor (PMSM) drives using Fundamental Excitation. The block diagram is also developed to study the speed of both sensor and sensorless PMSM drives. Furthermore, this project aims to show that sensorless system is comparable with system with sensor and it can reduce the cost of the drive.

CHAPTER 2

LITERATURE REVIEW

2.1 Introduction

This chapter discusses about the previous work conducted by other researchers to gain enough information that can be used to complete the project. All data are gathered related to the topic for this project which includes sources from books, journals, thesis and academic articles.

There are many studies that have been done regarding control of PMSM as permanent magnet motor is known for having compactness and high efficiency. In order to control a motor, the rotor position needs to be known. Therefore to obtain the rotor position, shaft sensor is used. However, in recent research sensorless control is introduced to replace the shaft sensor for its reliability and cheaper cost. There are a few method of sensorless control of PMSM drives that are widely use such as stator flux, Extended Kalman Filters (EKF) [20], sliding mode observer [23] and back electromotive force (BEMF)[19][10].

2.2 Back Electromotive Force (BEMF)

In [19], the study proposed the technique of a smooth transition strategy for back electromotive force (BEMF) sensorless PMSM control. It performs well under disturbance, high efficiency and without parameter requirement. Even though BEMF have dynamic response from middle to high speed region very well, it is also limited by too low BEMF at standstill and low speed. Thus position open loop constant current (I-F) starting method is used. I-F method is implemented to start the motor from standstill and drive it to low region. A novel smooth transition method is then used in the second part to switch the motor to field oriented control (FOC) based sensorless control, as it can drive the motor similar with sensor.

For this paper, the two methods used which are open loop and close loop control methods separated by speed loop topology. The problem with open loop topology is regarding its efficiency. However based on overview the close speed loop methods perform better dynamic response and robustness under rapid external disturbance. The BEMF based method can be used in all kind of PMSM regardless surface mount, internal mount or Direct-Current Brushless (DCBL). BEMF can be estimated by observer such as Kalman Filter or sliding mode observer. The switching procedure is as follow. Firstly, I-F drive the motor to a low speed, with a constant current (i^*_{q0}). If reference speed is greater than switching speed ($\omega^* \geq \omega^*_s$) , then current reference command should be decreased by switching law. Simultaneously the controller checks load angle ($\theta_L \leq \theta_{L0}$). If the condition occurs, the drive should be switched to sensorless FOC. The observer estimates the real rotor position angle by BEMF. The experimental results for this reference show that this method performs well at the switch point and FOC control with position feedback. Figure 2.1 shows the system structure of sensorless PMSM using BEMF

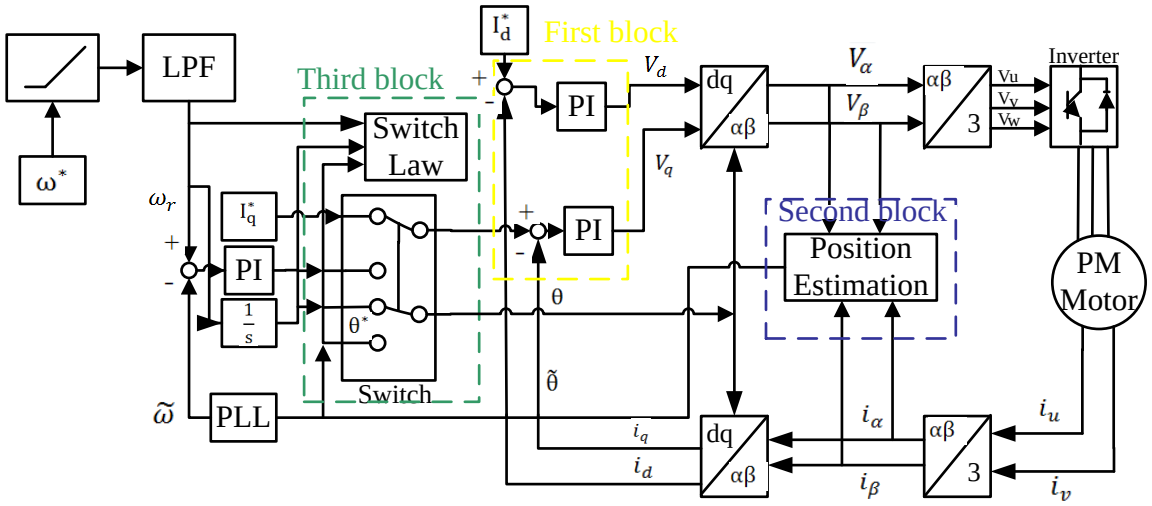

Figure 2.1: System structure of sensorless PMSM using BEMF [19].

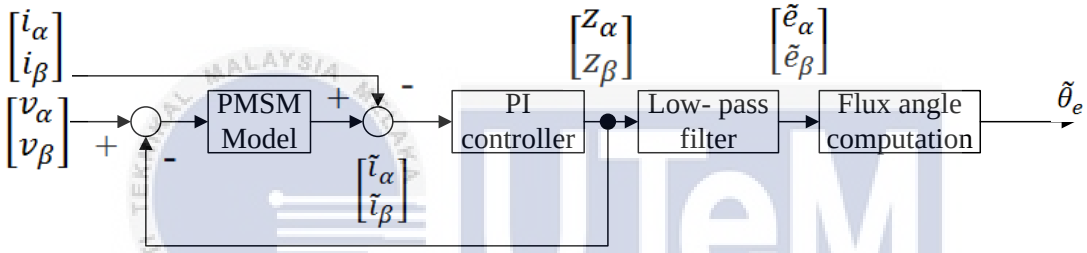

Figure 2.2: The structure of the position estimator [19].

While Figure 2.2 presents the structure of the position estimator. The position estimator uses the speed and voltage of alpha (α) and beta (β) as the input to produce output of position angle ($\tilde{\theta}$). The input first passes through PMSM model that is in direct and quadrature, which is 90 degree leading direct axis. The relationships is shown in (2.1) and (2.2)

$$\begin{bmatrix} V_d \\ V_q \end{bmatrix} = \begin{bmatrix} R_\alpha + pL_\alpha & -\omega_r L_\alpha \\ \omega_r L_\alpha & R_\alpha + pL_\alpha \end{bmatrix} \begin{bmatrix} i_\alpha \\ i_\beta \end{bmatrix} \begin{bmatrix} E_\alpha \\ E_\beta \end{bmatrix} \quad (2.1)$$

$$T_e = \frac{3}{2} P.\, i_q.\, (\varphi + (L_d - L_q).\, i_d) \quad (2.2)$$

Next is the observer controller also known as PI controller which is used to adjust the gain value, so that the needed value can be obtained by using the feedback. From the controller, it then passes through low pass filter and flux angle computation to gain the position angle. The algorithm of the sensorless motor control is deduced as in (2.3)

$$\begin{bmatrix} V_\alpha \\ V_\beta \end{bmatrix} = \begin{bmatrix} R_\alpha + pL_\alpha & 0 \\ 0 & R_\alpha + pL_\alpha \end{bmatrix} \begin{bmatrix} i_\alpha \\ i_\beta \end{bmatrix} \begin{bmatrix} E_\alpha \\ E_\beta \end{bmatrix} \tag{2.3}$$

E_α and E_β are the BEMF in $\alpha - \beta$ coordinate. The real rotor position angle is estimated by the BEMF observer in (2.4). Whereas for rotor angle between direct axis and phase axis are represented by θ and the angle is calculated using equation (2.5)

$$\begin{bmatrix} E_\alpha \\ E_\beta \end{bmatrix} = \omega_r \varphi \begin{bmatrix} -\sin\theta \\ \cos\theta \end{bmatrix} \tag{2.4}$$

$$\tilde{\theta} = \tan^{-1}\left(-\frac{E_\alpha}{E_\beta}\right) \tag{2.5}$$

Using the relationship from (2.6) the rotor angle speed (ω_r) can be obtained in (2.7)

$$\theta_L = \tilde{\theta} - \theta^* \tag{2.6}$$

$$\theta^* = \int \omega_r \, dt \tag{2.7}$$

where

θ_L = Load angle

θ^* = Command position locating in d^*-q^* reference frame

Other than that, Urbanski [22] also proposed the method of EMF by using a simple and effective structure of an observer. The structure is based on a modified concept of back EMF detection and it contains a corrector with a proportional-multi integral function. The observer system calculates position information from back EMF estimated in the $\alpha\beta$ coordinates to achieve position and speed information. Luenberger observer is use for this system. The operation concept of this observer is it performed correction based on error between calculated and measured current value. Besides that, observer operates well with longer simulating time and it uses a more complex corrector function that differ from the traditional one. The modelling of the control system includes a vector control system of stator current, a speed controller and a model of the observer. From simulation, it proof that sensorless mode drives have good performance at low speed. The structure of sensorless drive model and the general structure of observer are shown in Figure 2.3 and Figure 2.4 below respectively.

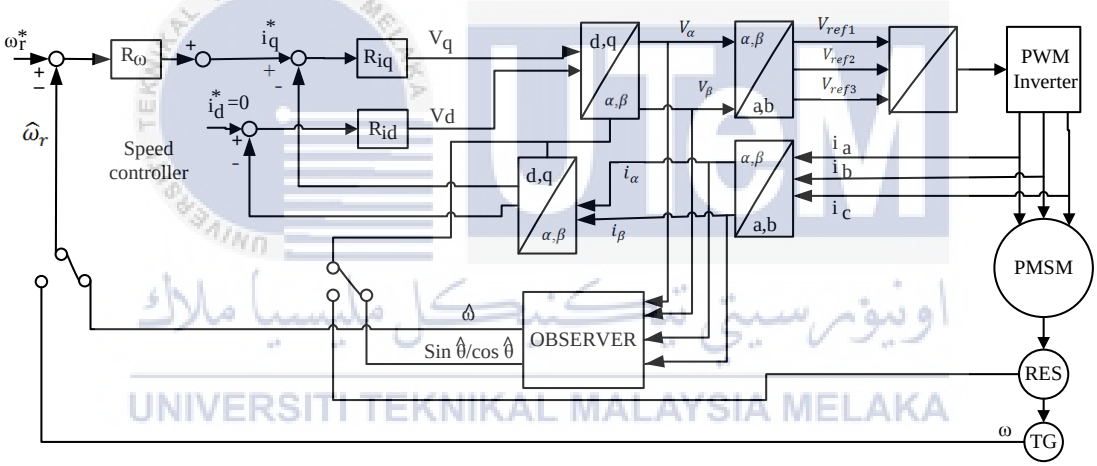

Figure 2.3: Structure of sensorless drive

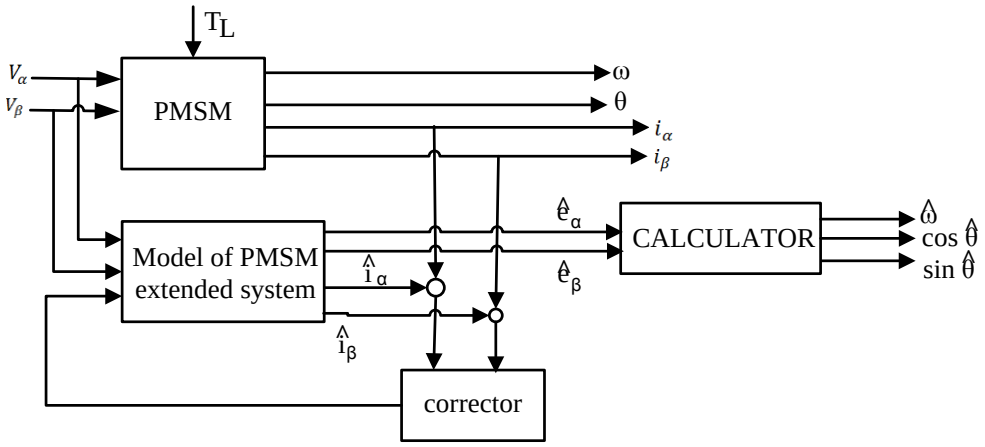

Figure 2.4: The general structure of observer

The position and speed estimation is expressed as follow

$$\sin\hat{\vartheta} = -\frac{\hat{e}_\alpha}{|\hat{e}|} \tag{2.8}$$

$$\cos\hat{\vartheta} = -\frac{\hat{e}_\beta}{|\hat{e}|} \tag{2.9}$$

Where

$|\hat{e}| = \sqrt{\hat{e}_\alpha^2 + \hat{e}_\beta^2}$

$|\hat{\omega}| = \frac{|\hat{e}|}{k_e}$

Carpaneto et al [24] proposed using BEMF for the speed and position estimation. The method used in here is similar to [19]. In order to ensure speed regulator stability a low pass filter is implemented. Even though the system is known to be sensorless, a sensor is used on the DC–link and estimating motor phase currents. In acquiring dc-link current and estimate motor phase currents the time t1 or t2 cannot be less than $10\mu s$. Beside field weakening algorithm which is use to widen motor speed range over the base speed, FOC strategy is also implemented to regulate motor speed and field weakening algorithm is also implemented. At first, current estimator runs and it is followed by BEMF. Steps taken for simulation first is run current estimator and followed by BEMF estimator. Then speed and voltage regulation, feed-forward calculation and current regulation precede the space vector modulation. Lastly, dc-link current acquisition times are calculated. From

simulation, it can be said that all the operating condition work in ac correct behaviour. The advantage of the BEMF estimation is that this method provides a simple step to deduce rotor position. The angle and speed estimation is expressed as

$$\theta = arctan\frac{E_\beta}{E_\alpha} \pm \frac{\pi}{2} \tag{2.10}$$

$$\omega_j = \frac{\theta(n)-\theta(n-1)}{Tc} \tag{2.11}$$

2.3 Extended Kalman Filter

Extended Kalman Filter (EKF) usage is proposed by Kung et al.[20]. Generally EKF is known as a full-order stochastic observer for the recursive optimum state estimation of a nonlinear dynamics system in real time by using signals that have disturbed with noise [21]. EKF can directly estimate the angular speed and has high convergence rate which give a more rapid speed response. However it needs heavy on-line 4x4 matrix computing that become a challenge for a fix pointed processor system. The problem can be solved by using Digital Signal Processor (DSP) or Filed Programmable Gate Array (FPGA). Comparing both, FPGA is a better option for the implementation of the digital system with programmable hard-wired feature, fast computation ability, low power consumption and higher density. The system consists of PMSM, EKF algorithm, SVPWM, speed controller and PI controller. To model the EKF algorithm a finite state machine (FSM) is used. The overall computation is carry out by manipulating 136 steps machine and the steps are explain in table 2.1 below.

Table 2.1: The description of the steps.

Steps	Description
$s_0 - s_{12}$	Calculate using Jacobian matrix and predict state variables
$s_{13} - s_{83}$	Perform the computation of temporary covariance matrix;
$s_{84} - s_{125}$	Calculate state error, update of the present covariance matrix and calculate the Kalman gain (Kn)
$s_{126} - s_{135}$	The computation of rotor flux position and rotor speed is carry out

From simulation results, this paper prove that the use of EKF in sensorless PMSM drive can accurately estimate the rotor flux position and rotor speed, as well as giving a good step response performance in case of low speed control, inverse speed control and high speed control. Figure 2.5 show the block diagram of the system.

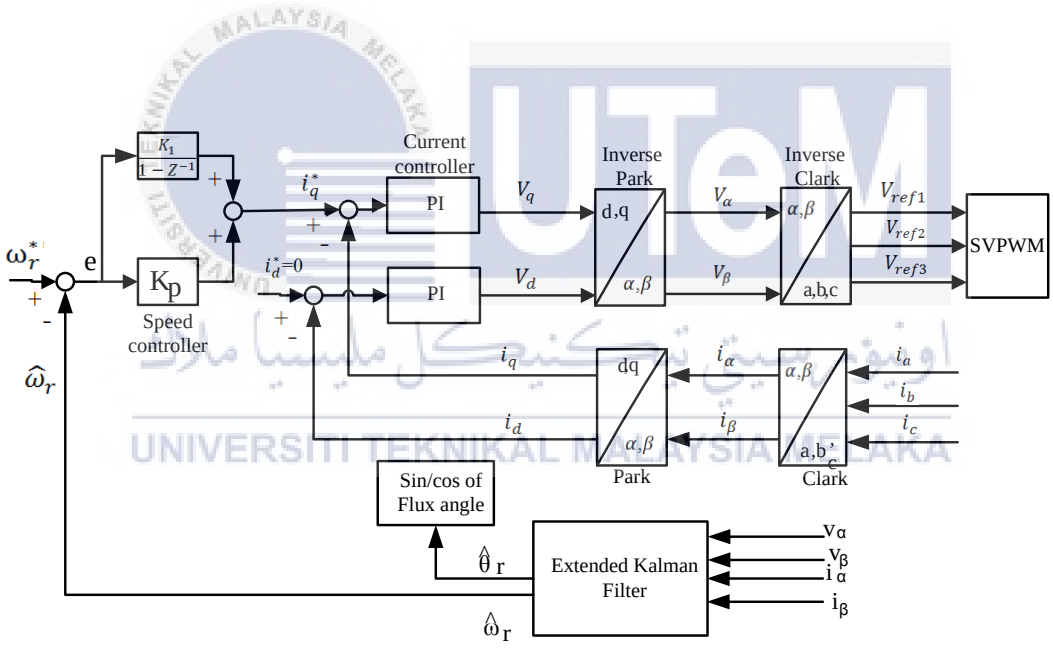

Figure 2.5: Block diagram using EKF for sensorless PMSM speed control system [20]

2.4 Sliding Mode Observer

Han et al [23] proposed a new speed and position sensorless control of the PMSM using sliding mode observer which include the Lyapunov algorithm to estimate the rotor speed and the stator resistance. The use of Lyapunov algorithm is proposed to overcome sensitivity problem cause by motor parameter variation. The system consists of a 400 W eight pole PMSM, DC generator and three phase inverter. The entire algorithms used are implemented using a TMS320C31. From simulation it shows that the real and estimated for both speed and position value are near which means that this method was very effective. The block diagram in Figure 2.6 shows the proposed algorithm.

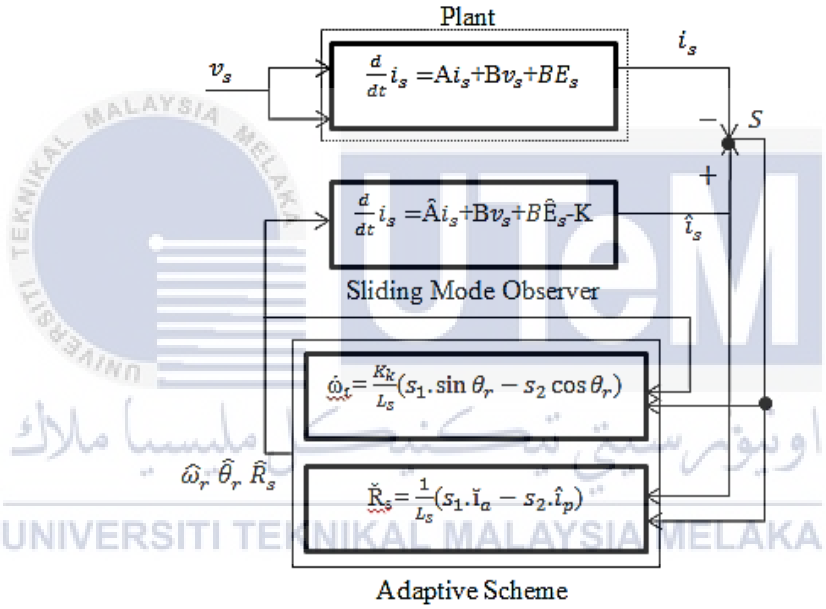

Figure 2.6: The proposed algorithm block diagram using sliding mode observer [23].

2.5 Stator Flux

Perera PD Chandana [10] proposed method of stator flux linkage vector. The stator flux linkage vector is estimated using stationary reference frame voltage. In order to estimate flux the stator phase voltage, current and stator resistance must be known. For this paper the method is used to calculate the 3 phase stator current. The difference between actual and calculated current is used to correct the assume rotor position. This can be

applied for PMSM. The disadvantage is initial rotor position is not detectable. The proposed block diagram using stator flux is shown in Figure 2.7 below

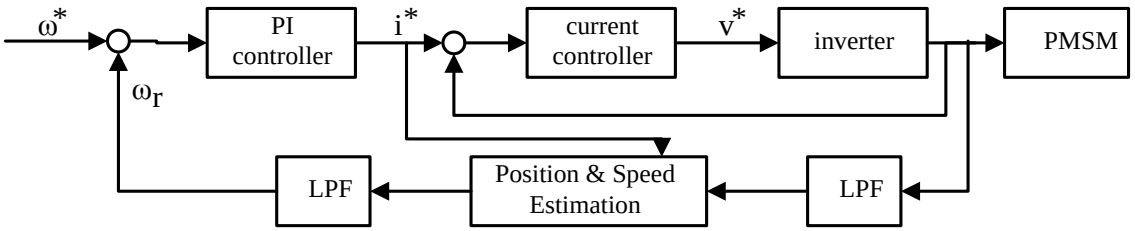

Figure 2.7: The proposed block diagram using stator flux

The motor speed and position is estimated as follows:

$$\hat{\omega}_e = \frac{\sqrt{\left(\frac{d\hat{\lambda}_\alpha}{dt}\right)^2 + \left(\frac{d\hat{\lambda}_\beta}{dt}\right)^2}}{\sqrt{\hat{\lambda}_\alpha^2 + \hat{\lambda}_\beta^2}} \quad (2.12)$$

$$\hat{\theta}_e = \hat{\theta}_e(0) + \hat{\omega}_e \mathrm{dt} \quad (2.13)$$

2.6 Summary of Literature Review

Based on the literature studies, this current study uses speed and position estimator using adaptive controller technique. This technique is selected as the sensorless technique for PMSM drives because it uses simple equation and system structure. Other technique uses long and complex equations which are hard to understand and modelled. The equation, structure and model of the selected technique are further discussed in chapter 3.

CHAPTER 3

METHODOLOGY

3.1 Introduction

This chapter covers about the methodology used to design and analyse the sensorless permanent magnet synchronous machine. Explanation regarding permanent magnet drive system and modelling of space vector pulse width modulation is also discussed. The development and simulation Simulink of the block diagram are presented with explanation as well.

3.2 Modeling of Permanent Magnet Drive System

This sub-chapter discusses the detail modelling of a permanent magnet synchronous motor. Topic explains about modelling of permanent magnet synchronous motor, permanent magnet motor control and PM motor control speed.

3.2.1 Modelling of PMSM

Modelling of permanent magnet motor drive system is essential to carry out proper simulation of the system. The d-q model shown in Figure 3.1 is developed on rotor reference frame. Rotation of rotor d-axis with fixed stator axis creates the angle, while the rotation of stator mmf with rotor d-axis creates the angle α [25]. The rotation can be at any given time.

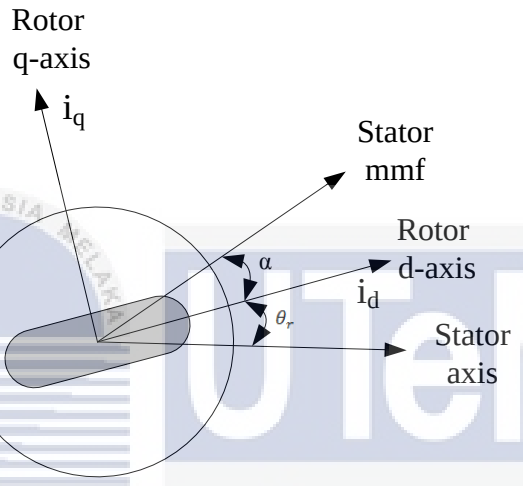

Figure 3.1: d-q coordinate system [28]

The PMSM model is build up using the following assumptions [25]:

1. Neglect the saturation.
2. The induced EMF is sinusoidal.
3. Neglects the eddy current and hysteresis losses.
4. There are no field current dynamic.

The mathematical model for a PMSM in d-q references frame is determined by using the following voltage, flux linkage and mechanical torque equation [29]

$$v_{dA} = r_{sA} i_{dA} + \frac{d}{dt}\varphi_{dA} - \omega_e \varphi_{qA} \tag{3.1}$$

$$v_{qA} = r_{sA} i_{qA} + p\varphi_{qA} - \omega_e \varphi_{dA} \tag{3.2}$$

Where:

v_d, v_q : *d-q* axis voltage

i_d, i_q : *d-q* axis currents

ω_e : electrical speed of motor

r_s : stator resistance

φ_d,φ_d : d-q axis flux linkages

The flux linkage can be expressed in the form of constant flux linkage φ_m and stator current due to rotor permanent magnet as in (3.3) (3.4):

$$\varphi_{dA} = L_{dA} i_{dA} + \varphi_{mA} \tag{3.3}$$

$$\varphi_{qA} = L_{qA} i_{qA} \tag{3.4}$$

Where

L_d, L_q : *d-q* axis inductances

By substituting equation (3.3) and (3.4) into (3.1) and (3.2), the equation for voltage is as below:

$$v_{dA} = r_{sA} i_{dA} + L_{dA} \frac{d}{dt} i_{dA} - \omega_e L_{qA} i_{qA} \tag{3.5}$$

$$v_{qA} = r_{sA} i_{qA} + L_{qA} \frac{d}{dt} i_{qA} + \omega_e L_{dA} i_{dA} + \omega_e \varphi_{mA} \tag{3.6}$$

The electromagnetic torque is expressed as

$$T_{em\,A} - T_{LA} = J \frac{d\theta_A}{dt} \tag{3.7}$$

$$T_{em\,A} = \frac{3}{2} p \times real\,\{i_A \varphi_{rA}\} \tag{3.8}$$

The instantaneous angular position is:

$$\omega_{rA} = \frac{d\theta_A}{dt} \tag{3.9}$$

I. d-q Modelling

The purpose of d-q modelling is to analyse the transient and steady state of motor. It is carried out by converting current and voltage three phase to a-b-c or d-q coordinate system using Park transformation [6]. Below is the equations use to convert the coordinate system.

Convert V_{abc} to V_{dq}

$$\begin{bmatrix} V_q \\ V_d \\ V_o \end{bmatrix} = \frac{2}{3}\begin{bmatrix} cos\,\theta_r & cos(\theta_r - 120) & cos(\theta_r + 120) \\ sin\,\theta_r & sin(\theta_r - 120) & sin(\theta_r + 120) \\ \frac{1}{2} & \frac{1}{2} & \frac{1}{2} \end{bmatrix}\begin{bmatrix} V_a \\ V_b \\ V_c \end{bmatrix} \tag{3.10}$$

Convert V_{dq} to V_{abc} :

$$\begin{bmatrix} V_a \\ V_b \\ V_c \end{bmatrix} = \frac{2}{3}\begin{bmatrix} cos\,\theta_r & sin\,\theta_r & 1 \\ cos(\theta_r - 120) & sin(\theta_r - 120) & 1 \\ cos(\theta_r + 120) & sin(\theta_r + 120) & 1 \end{bmatrix}\begin{bmatrix} V_q \\ V_d \\ V_o \end{bmatrix} \tag{3.11}$$

II. Equivalent Circuit of Permanent Magnet Synchronous Motor

The equivalent circuit of the motor as shown in Figure 3.2 will be used in simulation and study of motors. The circuit is derived from the voltage equations.

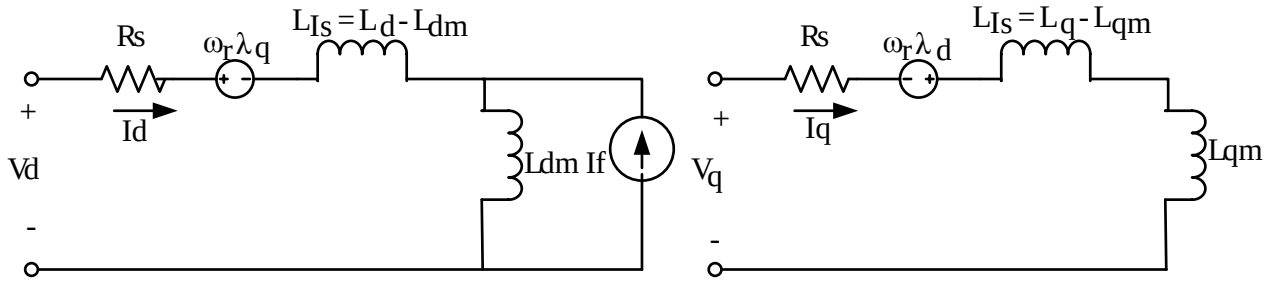

Figure 3.2: Permanent Magnet Synchronous Motor equivalent circuit [28].

3.2.2 PM Motor Control

Usually for operation of synchronous motor the control of PM motors are carried out by using field oriented control. The inverter is connected at the stator winding of the motor. The motor then produce variable value of voltage and frequency. Estimator that replaces the position sensor will control the output wave of the frequency and phase as shown in Figure 3.3.

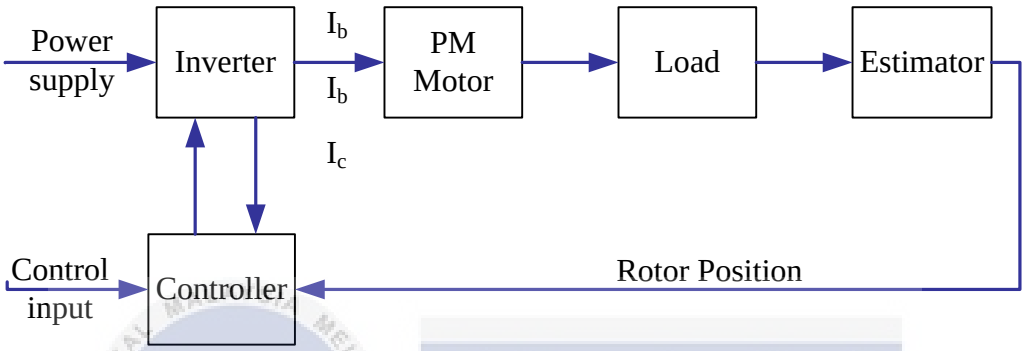

Figure 3.3: Estimator control synchronous motor [28]

I. Field Oriented Control of PM Motors

PMSM uses vector control or also known as field oriented control. The vector control uses direct current which equal to zero ($i_d = 0$), to obtain a 90 degree difference between direct and quadrature (d-q) axis [26]. Field oriented controls indicate that synchronous motor could be handled like a separately excited dc motor. It is achieved, by knowing the permanent magnet rotor position or the instantaneous rotor flux position. However it requires an encoder or resolver. The three phase current is gained by calculation but only after the position is known. In this project, the control option used is the constant torque. The vector control system have different loop which are feedback, position and speed loop. Excitation and PMSM torque is controlled by the current loop. The stator current gain from the output of inverter is transformed into rotor speed using Park transformation. Torque and excitation component can be adjusted using PI controller.

The output of the controller is then passes through Park Inverse and fed to the SVPWM and inverter.

a. Constant torque

The constant torque control strategy is derived from vector control, which the required condition at all time is maximum possible torque. It is executed by setting the torque producing current (iq) equivalent to the current supply (I_m). The angle used is 90 degree. By setting the i_d current value to zero the torque equation is:

$$T_e = \left(\frac{3}{2}\right)\left(\frac{p}{2}\right)\lambda_f i_q \tag{3.12}$$

Assume that

$$k_t = \left(\frac{3}{2}\right)\left(\frac{p}{2}\right)\lambda_f \tag{3.13}$$

The torque is given by

$$T_e = k_t i_q \tag{3.14}$$

3.2.3 PM Motor Speed Control

Speed control system is used to set and modify the speed of a motor. The system consists of motor, inverter, controller, speed setting device and feedback systems. The aim of motor speed controller is to drive the motor towards the speed demand. Advantage of a closed loop speed control system is fast response, but it requires feedback element which is expensive.

I. Speed Control Loop Implementation

The system of PM motor drive consists of a motor, inverter, controller with constant torque operation. Block diagram of the system is shown in Figure 3.4. The controller operates based on range of speed. If speed exceeds rated speed, it runs in flux weakening area and vice versa. However since direct current set to zero ($i_d = 0$), the controller will only operate in constant torque area [26].

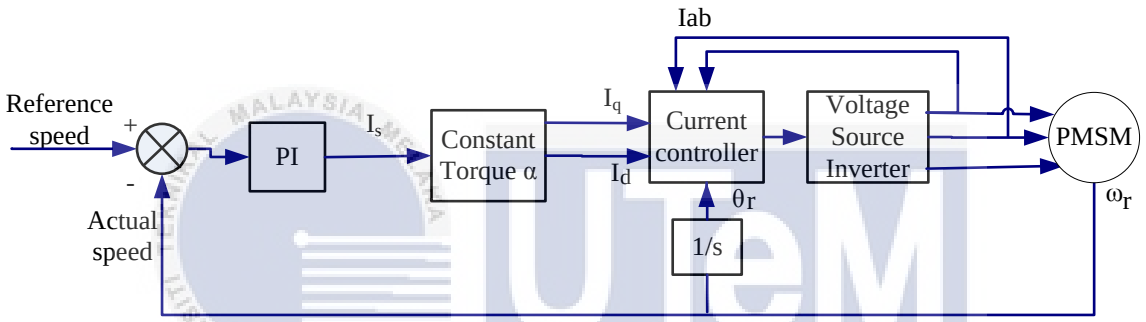

Figure 3.4: Block diagram of system [28]

Figure 3.4 presents the block diagram of the system. It starts with taking in reference speed and actual speed as the input. Then both the speed are compared which produce error as the output. After that, the error is fed to the PI controller that produces current. Direct current (i_d) is set to zero, to make the angle between direct and quadrature current equals to 90 degree. Next, is the voltage source inverter that acts as switching which is use in the PMSM. The output of PMSM which is the actual speed is used as feedback to the system. The integration from the actual speed produce angle and is inserted to current controller. The flow of the process is shown in Figure 3.5.

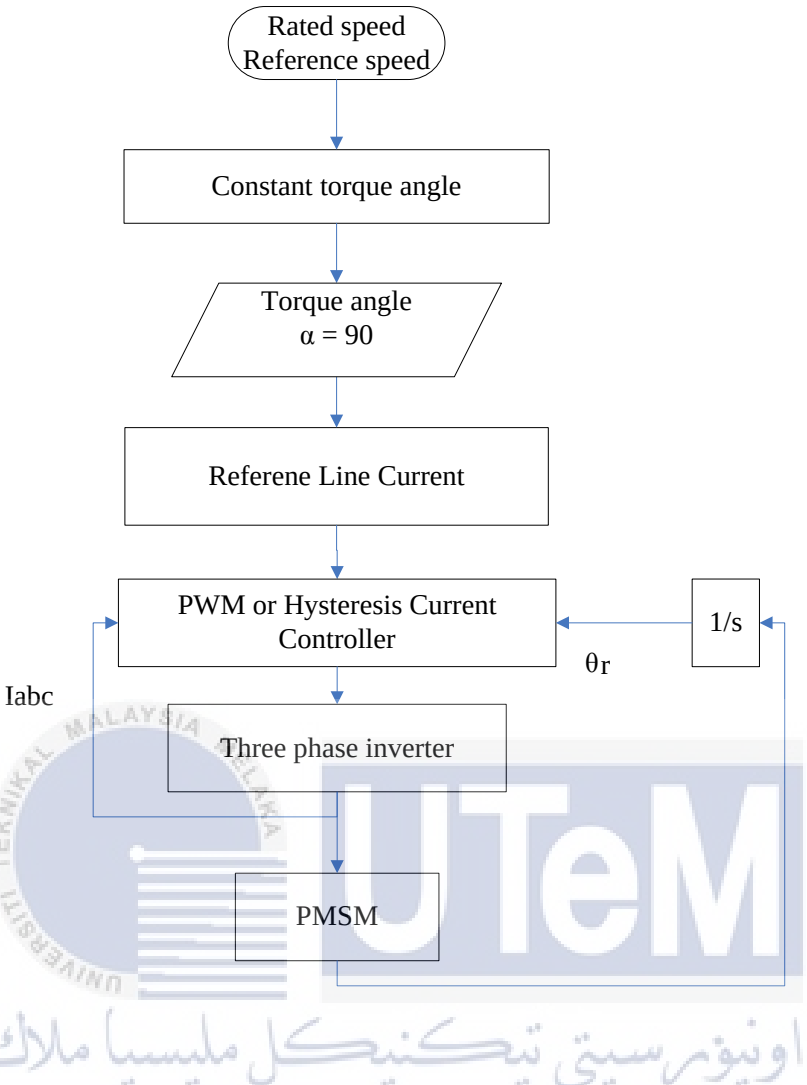

Figure 3.5: Flow of system drive

Figure 3.5 shows the flow of system drive simplified from Figure 3.4. Firstly speed is taken as the input. Speed controller produces error value which is fed to PI controller. The error is obtained by comparing the actual and reference speed. The integration of speed produces torque as outcome and the torque angle is set to 90 degree. After that current is fed to the pulse width modulation (PWM) to produce switching signal which is the used in the inverter. From the PMSM, actual speed is obtained and then integrated to obtained angle rotor position. The angle is adjusted to control the switching of pulse width modulation.

3.3 SVPWM

SVPWM is a unique switching sequence based on the top three power transistors of inverter. The output voltage and current is proven to have less harmonic distortion. Comparing it with sinusoidal modulation technique, SVPWM give out a more productive use of voltage supply as shown in Figure 3.6 [27]. SVPWM is widely used to vary frequency and speed regulation. It is obtained by controlling the motor using eight switch status of the space voltage vector to variable the frequency of speed and voltage adjustment. The switching of space voltage vector will provide circular rotation of magnetic field. Therefore the inverter is controlled to get a specific output of voltage waveform. In simple words the aim of SVPWM is to develop a voltage vector that is near to the reference value through different switching modes of inverter [17]. Benefit of using SVPWM is to reduce total harmonic distortion (THD) created by rapid switching of inverter.

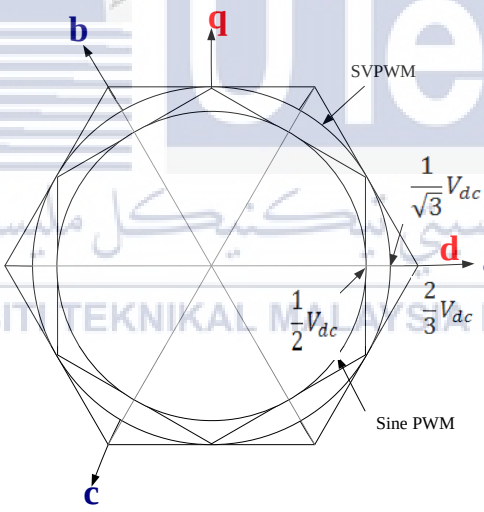

Figure 3.6: Sine PWM and SVPWM locus comparison [27]

The voltage equation can be transform from abc to d-q reference frame which is made up of direct and quadratur axis as shown in Figure 3.7. The d-axis is placed horizontally and vertically for q-axis.

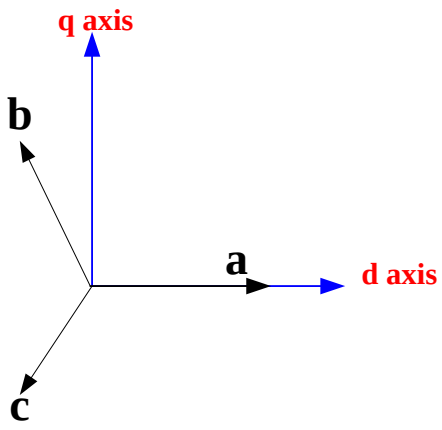

Figure 3.7: Relationship between abc and dq reference frame [27].

3.3.1 Principal of SVPWM

Basic circuit design is shown in Figure 3.8. The output of inverter is determine using the six switches S_1 to S_6. The switch condition 'ON 'and 'OFF' is represent by 1 and 0 which refer to the upper switches. Upper and lower switches cannot operate at the same time otherwise it becomes short circuit. There is a total of eight switch status in which two of it has zero vectors (V_0,V_7) and the other vectors are (V_1, V_2, V_3, V_4, V_5,V_6) as shown in Figure 3.9.

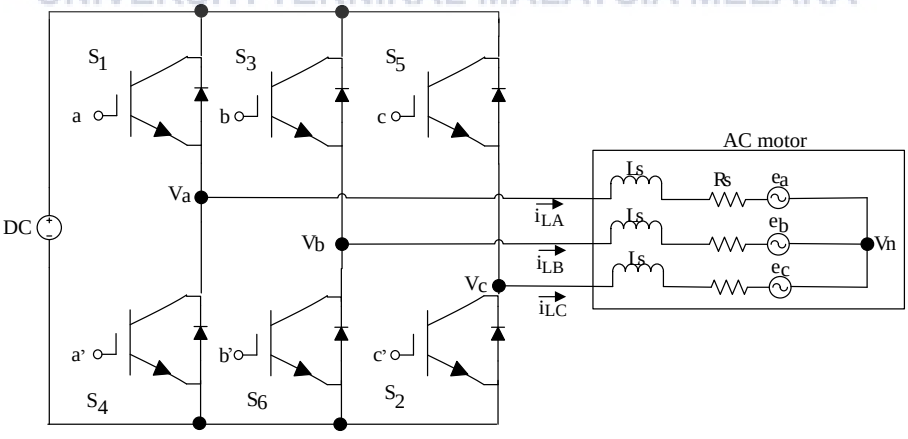

Figure 3.8: Three phase voltage source PWM inverter [29]

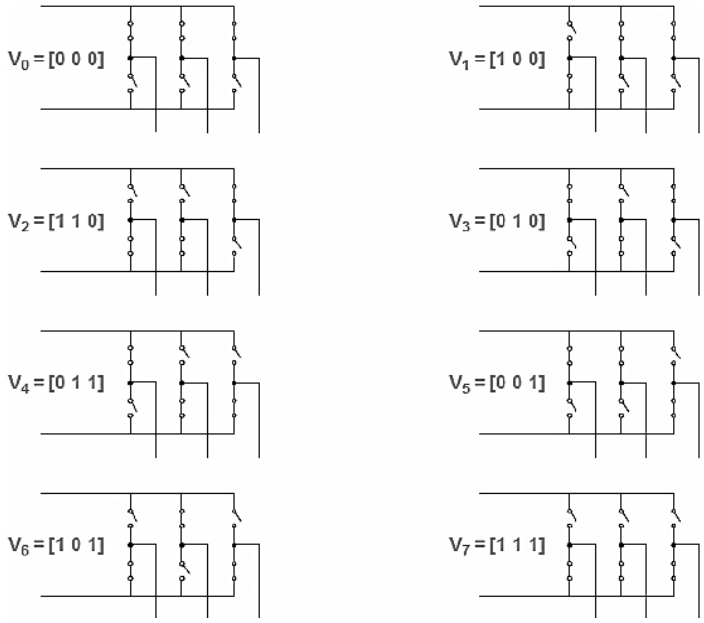

Figure 3.9: The inverter voltage vector [29]

The relationship of switching vector and line-to-line voltage vector is shown in 3.15

$$\begin{bmatrix} V_{ab} \\ V_{bc} \\ V_{ca} \end{bmatrix} = V_{dc} \begin{bmatrix} 1 & -1 & 0 \\ 0 & 1 & -1 \\ -1 & 0 & 1 \end{bmatrix} \begin{bmatrix} a \\ b \\ c \end{bmatrix} \quad (3.15)$$

The relationship of switching vector and line-to-line voltage vector is shown in 3.16

$$\begin{bmatrix} V_{an} \\ V_{bn} \\ V_{cn} \end{bmatrix} = \frac{V_{dc}}{3} \begin{bmatrix} 2 & -1 & 1 \\ -1 & 2 & -1 \\ -1 & -1 & 2 \end{bmatrix} \begin{bmatrix} a \\ b \\ c \end{bmatrix} \quad (3.16)$$

The aim of SVPWM technique is to estimate the reference voltage (Vref) by applying the eight switching state. Refer Figure 3.10. A technique of approximation is to produce the output average similar with the reference voltage in the same interval.

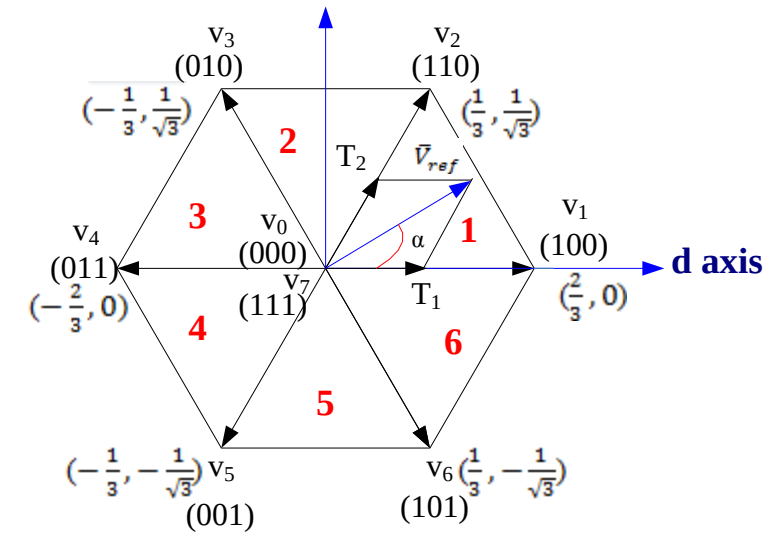

Figure 3.10: Basic switching vectors and sector [29]

3.3.2 Implementation of SVPWM

The steps to implement the SVPWM are:

- Step 1: Determine V_d, V_q, V_{ref}, and angle (α)
- Step 2: Determine time duration T1, T2, T0
- Step 3: Determine the switching time of each transistor (S1 to S6)

a. Determining voltage (V_d, V_q, V_{ref}) and angle (α)

The value of angle, voltage reference and voltage at d and q axis is calculated using formula as follow. Refer Figure 3.11.

$$\begin{bmatrix} V_q \\ V_d \end{bmatrix} = \frac{2}{3}\begin{bmatrix} 1 & -\frac{1}{2} & -\frac{1}{2} \\ 0 & \frac{\sqrt{3}}{2} & -\frac{\sqrt{3}}{2} \end{bmatrix}\begin{bmatrix} V_{an} \\ V_{bn} \\ V_{cn} \end{bmatrix} \tag{3.17}$$

$$[Vref] = \sqrt{{V_d}^2 + {V_q}^2} \tag{3.18}$$

$$\alpha = tan^{-1}\left(\frac{V_q}{V_d}\right) = \omega t = 2\pi f t \quad (3.19)$$

Where:

α: Angle value

f: Fundamental frequency

V_{ref} : The reference voltage

The value of voltage at d and q axis is used to calculate the reference voltage. Angle α is also calculated in order to determine which sector the voltage reference is located. The sector is divided into six and angle between each angle is 60 degree as shown in Figure 3.10. If value of α range is $0° \leq \alpha < 60°$, V_{ref} is in sector 1. If value of α range is $60° \leq \alpha < 120°$, V_{ref} is in sector 2. If value of α range is $120° \leq \alpha < 180°$, V_{ref} is in sector 3. If value of α range is $180° \leq \alpha < 240°$, V_{ref} is in sector 4. If value of α range is $240° \leq \alpha < 300°$, V_{ref} is in sector 5. If value of α range is $300° \leq \alpha < 360°$, V_{ref} is in sector 6.

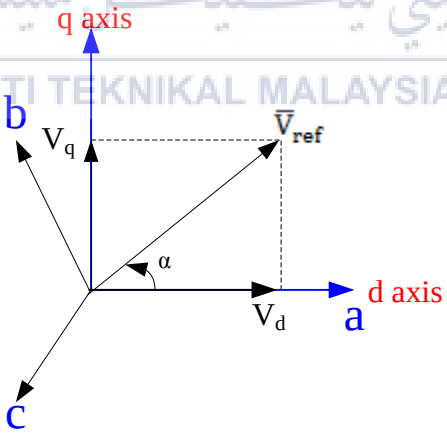

Figure 3.11: Voltage space vector diagram [27]

b. Determining time duration

By referring Figure 3.12, the switching time duration is determined as follows:

Switching time duration at Sector 1

$$T_z.V_{ref} = T_1.V_1 + T_2.V_2 \quad (3.20)$$

$$T_1 = T_z.\alpha.\frac{sin(\pi/3-\alpha)}{sin(\pi/3)} \quad (3.21)$$

$$T_2 = T_z.\alpha.\frac{sin(\alpha)}{sin(\pi/3)} \quad (3.22)$$

$$T_0 = T_z - (T_1 + T_2) \quad (3.23)$$

Switching time duration at any sector

$$T_z.V_{ref} = T_1.V_1 + T_2.V_2 \quad (3.24)$$

$$T_1 = \frac{V_{ref}.T_z.\sqrt{3}.}{V_{dc}}.\left(sin\left(\frac{\pi}{3}\alpha - \frac{n-1}{3}\pi\right)\right) \quad (3.25)$$

$$T_2 = \frac{V_{ref}.T_z.\sqrt{3}.}{V_{dc}}.\left(sin\left(\alpha - \frac{n-1}{3}\pi\right)\right) \quad (3.26)$$

$$T_0 = T_z - T_1 - T_2 \quad (3.27)$$

Where:

T_z: Sampling time

n: the value is 1

The symbol T_z represent the sampling time whereas T_0, T_1, T_2 are the vector time span. The duration for each voltage vector is obtained by using equation (3.20).

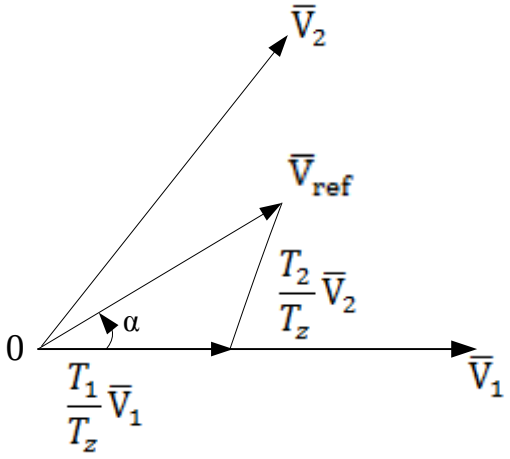

Figure 3.12: Reference vector at sector 1 [29].

c. Determining switching time

SVPWM is a method used to determine the switching sequence of the switches of the inverter. The three phase inverter is presented in Figure 3.13. Each inverter state corresponds to certain combination of switches. There are two switches in each leg of a two level inverter. The switches in one leg cannot be 'ON' at the same time as it will lead to short circuit. States are numbered using binary, 0 for 'OFF' and 1 for 'ON". The state refers to the upper switch. It result in 6 active switching vector (V_1, V_2, V_3, V_4, V_5, V_6) and 2 zero states (V_0, V_7) as shown Table 3.1 [18].

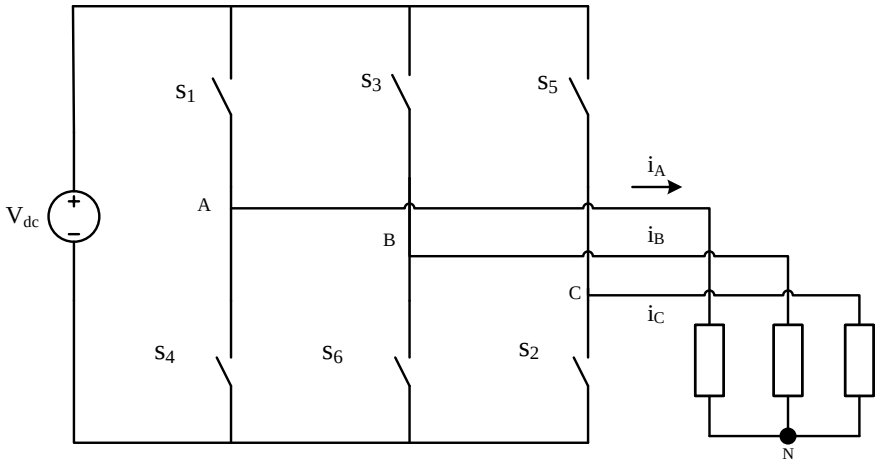

Figure 3.13: Three phase voltage source PWM inverter [18]

Table 3.1: Switching patterns and output vector

Space Vector	Switching State	Switching sector			'On' Switches
		A	B	C	
Zero vector	V_0	0	0	0	4,6,2
Active vector	V_1	1	0	0	4,6,5
	V_2	1	1	0	4,3,2
	V_3	0	1	0	4,3,5
	V_4	0	1	1	1,6,2
	V_5	0	0	1	1,6,5
	V_6	1	0	1	1,3,2
Zero Vector	V_7	1	1	1	1,3,5

The switching of the SVPWM can also be known or obtained by using calculation. The formula used for the calculation is as shown in Table 3.2 below. Each formula differs for each sector from sector 1 to sector 6. The upper switches include the S_1, S_3 and S_5. While the lower switches consists of switch S_2, S_4 and S_6.

Table 3.2: The switching time

Sector	Upper Switches (S_1, S_3, S_5)	Lower Switches (S_2, S_4, S_6)
1	$S_1 = T_1 + T_2 + T_0/2$ $S_3 = T_2 + T_0/2$ $S_5 = T_0/2$	$S_2 = T_1 + T_2 + T_0/2$ $S_4 = T_0/2$ $S_6 = T_2 + T_0/2$
2	$S_1 = T_1 + T_0/2$ $S_3 = T_1 + T_2 + T_0/2$ $S_5 = T_0/2$	$S_2 = T_1 + T_2 + T_0/2$ $S_4 = T_2 + T_0/2$ $S_6 = T_0/2$
3	$S_1 = T_0/2$ $S_3 = T_1 + T_2 + T_0/2$ $S_5 = T_2 + T_0/2$	$S_2 = T_1 + T_0/2$ $S_4 = T_1 + T_2 + T_0/2$ $S_6 = T_0/2$
4	$S_1 = T_0/2$ $S_3 = T_1 + T_0/2$ $S_5 = T_1 + T_2 + T_0/2$	$S_2 = T_2 + T_0/2$ $S_4 = T_1 + T_2 + T_0/2$ $S_6 = T_0/2$
5	$S_1 = T_2 + T_0/2$ $S_3 = T_0/2$ $S_5 = T_1 + T_2 + T_0/2$	$S_2 = T_0/2$ $S_4 = T_1 + T_0/2$ $S_6 = T_1 + T_2 + T_0/2$
6	$S_1 = T_1 + T_2 + T_0/2$ $S_3 = T_0/2$ $S_5 = T_1 + T_0/2$	$S_2 = T_2 + T_0/2$ $S_4 = T_0/2$ $S_6 = T_1 + T_2 + T_0/2$

3.4 Sensorless Control

Recently, most permanent magnet motor uses sensorless control to obtain the rotor position because it reduces system cost and complexity [10]. Hence, rotor position and velocity estimation technique is discussed in this part. The parameter that needs to be measure for the position and velocity is motor phase currents.

3.4.1 Velocity Estimation and Rotor Position

One of the sensorless techniques is the velocity estimation and rotor positioning. The currents of the stator are being approximate at an expected rotor position by using estimated stator flux obtained. After this step, values of current errors are obtained by comparing the measured currents and estimated stator current. The algorithm of block diagram is shown in Figure 3.14

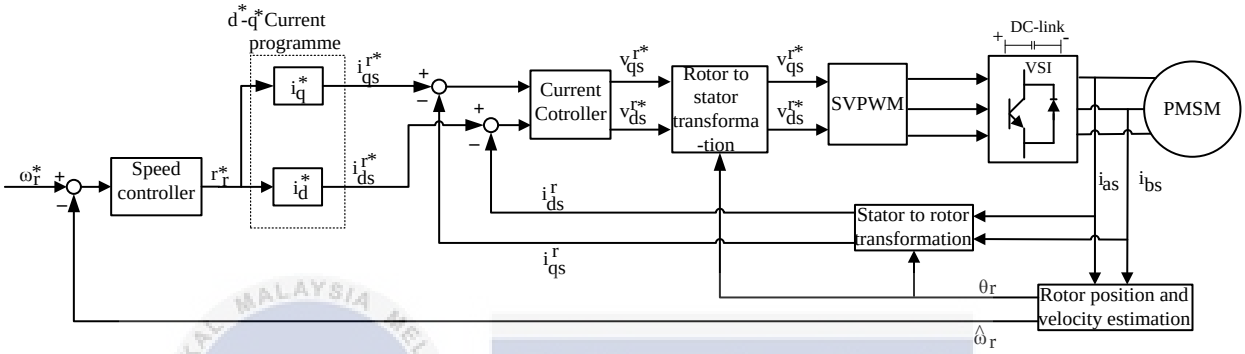

Figure 3.14: The sensorless rotor permanent magnet flux oriented controlled drive system block diagram [10]

There are five step in obtained the rotor position and velocity estimation. The steps involved are estimation of stator flux linkage, estimation of stator current, position correction, flux linkage update and rotor position prediction

i. Estimation of stator flux linkage

Firstly, the ohmic voltage drop and stator voltage difference is being integrated to get the estimated stator flux linkage. Equation below is used to acquire the stator flux linkage.

$$\hat{\lambda}_{qs}^{s}(k) = T\left[v_{qs}^{s*}(k-1) - r_s i_{qs}^{s}(k)\right] + \lambda_{qs}^{s}(k-1) \tag{3.28}$$

$$\hat{\lambda}_{ds}^{s}(k) = T[v_{ds}^{s*}(k-1) - r_s i_{ds}^{s}(k)] + \lambda_{ds}^{s}(k-1) \tag{3.29}$$

Where:

T: Sampling time

k: the sampling number

λ_{ds}^{s}: flux value

Next, to calculate values of the stator flux in the latest sampling period the new flux value obtained are used. Transformation of two phase stationary reference current from measured phase current is done to obtained value of i_{ds}^{s} and i_{qs}^{s}. The voltages used in flux equation above are commanded by the controller to the system. In order to calculate the stator flux values in the present sampling period, updated flux values gained from the previous sampling are used in (3.28) and (3.29).

ii. Estimation of stator current

The second step is estimating the stator current. In order to obtain the stator current, the predicted rotor position and the estimated flux that is gained from the first step are used. Where the stator currents estimation are expressed as

$$\hat{\imath}_{qs}^{s}(k) = \frac{\left[L-\Delta L\cos\left(2\hat{\theta}_{rp}(k)\right)\right]\hat{\lambda}_{qs}^{s}(k)+\Delta L\sin\left(2\hat{\theta}_{rp}(k)\right)\hat{\lambda}_{ds}^{s}(k)-(L-\Delta L)\lambda_{m}\sin(\hat{\theta}_{rp}(k))}{L^{2}-\Delta L^{2}} \quad (3.30)$$

$$\hat{\imath}_{ds}^{s}(k) = \frac{\left[L+\Delta L\cos\left(2\hat{\theta}_{rp}(k)\right)\right]\hat{\lambda}_{ds}^{s}(k)+\Delta L\sin\left(2\hat{\theta}_{rp}(k)\right)\hat{\lambda}_{qs}^{s}(k)-(L+\Delta L)\lambda_{m}\sin(\hat{\theta}_{rp}(k))}{L^{2}-\Delta L^{2}} \quad (3.31)$$

Where, L: $\frac{L_q+L_d}{2}$ and ΔL: $\frac{L_q-L_d}{2}$

iii. Position correction

In step 3 is the predicted rotor position correction. It is gained by calculating the difference between the actual current and estimated current. The equation is in (3.32) and (3.33)

$$\Delta i_{qs}^{s}(k) = i_{qs}^{s}(k) - \hat{\imath}_{qs}^{s}(k) \tag{3.32}$$

$$\Delta i_{ds}^{s}(k) = i_{ds}^{s}(k) - \hat{\imath}_{ds}^{s}(k) \tag{3.33}$$

iv. Flux linkage update

Next in step 4, the flux linkage is updated. To update the flux linkage, the measured stator current and corrected rotor position are calculated again. These values of updated flux are used to estimate the flux in step one for the next sampling interval. Using this method the integrator drift problem in the flux estimation in step one is avoided. The equations used are as follow

$$\lambda_{qs}^{s}(k) = \left[L + \Delta L \cos\left(2\hat{\theta}_r(k)\right)\right] i_{qs}^{s}(k) - \Delta L \sin\left(2\hat{\theta}_r(k)\right) i_{ds}^{s}(k) + \lambda_m \sin(\hat{\theta}_r(k)) \tag{3.34}$$

$$\lambda_{ds}^{s}(k) = \left[L - \Delta L \cos\left(2\hat{\theta}_r(k)\right)\right] i_{ds}^{s}(k) - \Delta L \sin\left(2\hat{\theta}_r(k)\right) i_{qs}^{s}(k) + \lambda_m \cos(\hat{\theta}_r(k)) \tag{3.35}$$

v. Rotor position prediction

For the last step, the rotor position is predicted by assuming the position varies with time as a second order polynomial

$$\theta_r = At^2 + Bt + C \tag{3.36}$$

Assume t=0 at (k-2) sampling instant, the rotor position is obtained from (3.37)

$$\hat{\theta}_r(k-2) = C \tag{3.37}$$

At (k-1) sampling instant

$$\hat{\theta}_r(k-1) = AT^2 + BT + C \tag{3.38}$$

At (k) sampling instant

$$\hat{\theta}_r(k) = A(2T^2) + B(2T) + C \tag{3.39}$$

At (k) sampling instant the predicted position is

$$\hat{\theta}_{rp}(k+1) = A(3T^2) + B(3T) + C \tag{3.40}$$

By simplifying and substituting A, B and C to (3.42), the predicted rotor position at (k+1) sampling instant is expressed as

$$\hat{\theta}_{rp}(k+1) = 3\hat{\theta}_r(k) - 3\hat{\theta}_r(k-1) + \hat{\theta}_r(k-2) \tag{3.41}$$

3.4.2 Selected sensorless

This part discussed about the type of sensorless that is selected to be implement in this project.

3.4.2.1 Speed and Position Estimator using adaptive controller

The adaptive controller is designed to obtain actual speed using a few equations. Firstly the three phase voltage and current are converted to d-q model through park clark transformation as shown in Figure 3.15. The d-q is obtained using equation (3.42)

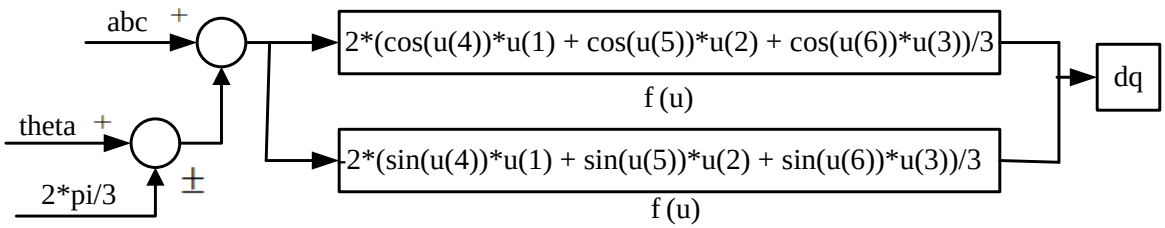

Figure 3.15: Park and Clark transformation block diagram

$$\begin{bmatrix} i_d \\ i_q \end{bmatrix} = \frac{2}{3}\begin{bmatrix} \cos\theta & \cos\left(\theta - \frac{2\pi}{3}\right) & \cos\left(\theta + \frac{2\pi}{3}\right) \\ -\sin\theta & -\sin\left(\theta - \frac{2\pi}{3}\right) & -\sin\left(\theta + \frac{2\pi}{3}\right) \end{bmatrix}\begin{bmatrix} i_a \\ i_b \\ i_c \end{bmatrix} \tag{3.42}$$

Then the d-q current and voltage is used in equation (3.43) and (3.44) which is formulated from equation (3.1) and (3.2).

$$\frac{d}{dt}\hat{i_d} = \frac{(V_d^* - r_s\hat{i_d} + \hat{\omega_e}L_q\hat{i_q})}{L_d} \tag{3.43}$$

$$\frac{d}{dt}\hat{i_q} = \frac{(V_q^* - r_s\hat{i_q} - \hat{\omega_e}L_d\hat{i_d} - \hat{\omega_e}\varphi_m)}{L_q} \tag{3.44}$$

The estimated d-q current which is the output of the Park and Clark transformation is then compared with actual d-q axis currents. These currents are used to calculate the estimated speed. It is calculated using Popov's hyper-stability theory to obtained the estimated speed equation in (3.45)

$$\hat{\omega_e} = \left(K_p \times \frac{K_i}{3}\right)g \tag{3.45}$$

$$g = \left(i_d \times \hat{i_q}\right) - \left(i_q \times \hat{i_d}\right) - \frac{\varphi_m}{L}\left(i_q \times \hat{i_q}\right) \tag{3.46}$$

Whereas the estimation error as shown in equation (3.46) is derived when the speed used in the model is not identical to the actual speed without any influence from variation of parameter. Generation from the regulation of this error through a PI controller is used as the tuning signal.

3.5 Block Diagram Design

This chapter presents the block diagram of sensorless PMSM drives using fundamental excitation. The block diagram presented includes speed estimator and Park and Clark transformation.

3.5.1 Speed Estimator Block Diagram

The block diagram for the speed estimator is in shown in Figure 3.16

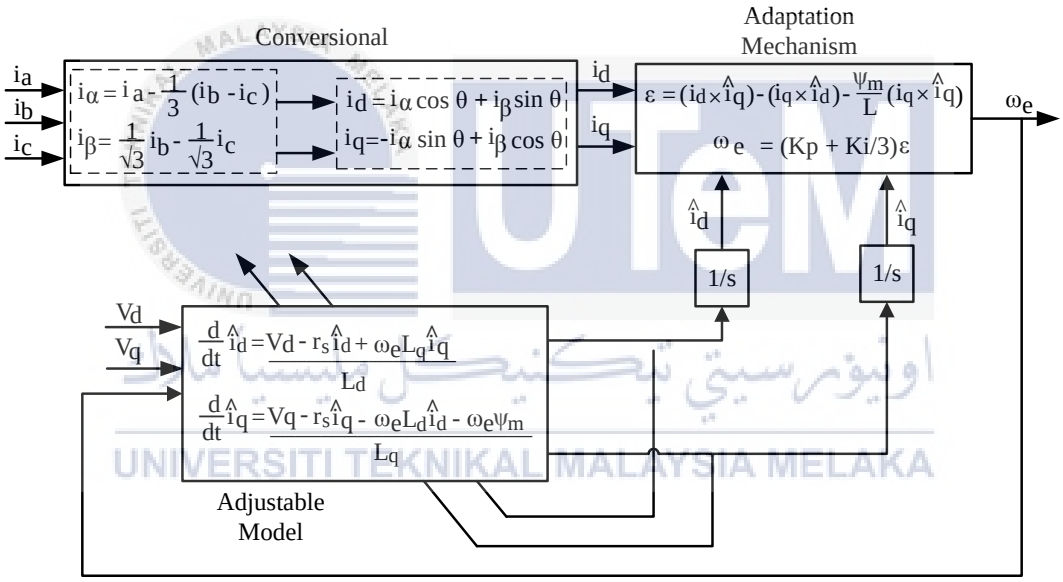

Figure 3.16: The estimator block diagram

Figure 3.16 presents the estimator block diagram that consists of three blocks which are conversional, adaptation mechanism and adjustable model. Firstly the three phase voltage and current are converted to d-q model through park clark transformation. The estimated d-q current which is the output of the Park and Clark transformation is then compared with actual d-q axis currents. Lastly, the speed is estimated from taking in current as the input. The speed is calculated using Popov's hyper-stability theory as shown in the adaptation mechanism.

3.6 Project Gantt Chart and key milestone

The milestones for this project are as follow:

Milestone 1- Research on PMSM motor drive and sensor..

Milestone 2- Model a PMSM motor drive system using PMSM.

Milestone 3- Study type of sensorless.

Milestone 4- Model and analyse the simulation performance sensorless using Simulink.

Milestone 5- Preparation of report and slide for presentation.

The Gantt chart in Table 3.3 shows the task conducted monthly, starting from September 2015 until May 2016. The first three month focuses on research on PMSM motor drive and sensor. All the information regarding motor drive and sensorless is gathered in chapter two. For the following two months development of PMSM model and SVPWM is carried out. On the next three month study in sensorless is done and a type of sensorless is selected. Next, simulation and analysis of the complete sensorless PMSM by using fundamental excitation is accomplished.

Table 3.3 : Gantt Chart

Milestone	Year	2015				2016				
	Task	9	10	11	12	1	2	3	4	5
1	Research on PMSM motor drive and sensor									
2	Model a PMSM motor drive system using PMSM									
3	Study type of sensorless									
4	Model and analyze the simulation performance sensorless using Simulink									
5	Preparation of report and slide for presentation									

3.6.1 Flowchart of Project

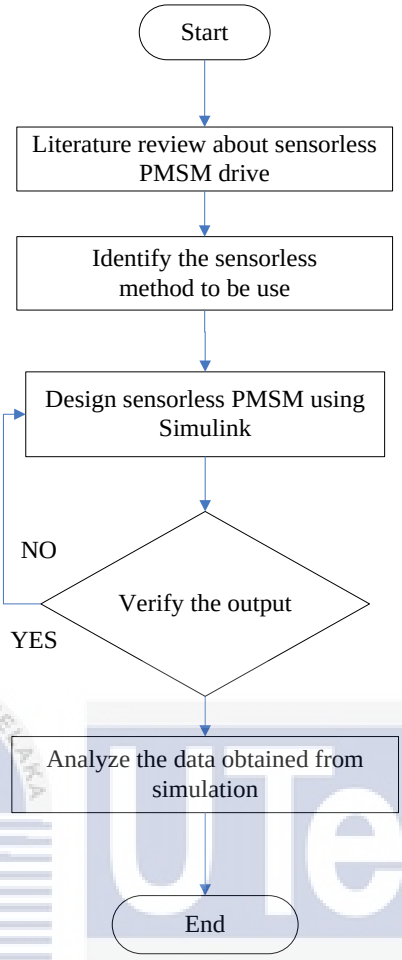

Figure 3.17: Flowchart of research methodology

Figure 3.17 shows the flowchart of the project research methodology. Firstly study of sensorless PMSM drive is carried out to prepare the literature review. After multiple type of sensorless is studied a sensorles method is selected to be used in this project. Then, the sensorless PMSM is designed using Simulink R2013a software and is tested. When the output after testing is not as wanted, the system design is rechecked. However if the output is good, data obtained from the simulation is analysed. Finally, after the completion of the modelling, the result of the measured value is compare with reference value to ensure that the motor drive can drive the value near to reference value.

CHAPTER 4

RESULT AND DISCUSSION

4.1 Introduction

The modelling of the simulation block for SVPWM, PMSM and estimator has been shown in the previous chapter, which is chapter 3. Thus, this chapter discussed the simulation result of the sensorless PMSM in terms of speed and current with different value of reference speed and also load variation.

4.2 Simulation Result

The simulation results for the sensorless PMSM by using fundamental excitation are presented in this section with different input reference speeds. The values used for the reference speed are 500 rpm, 1000 rpm and 1500 rpm. The DC voltage source supplies 300V and 50Hz. The designed PMSM parameters used are that pole pair is 4, resistance is 4.33Ω, inductance is 17.6mH, flux linkage is 0.194925V_s, friction factor is 0.0003Nms and inertia is 0.000881kgm^2.

4.2.1 Simulation Result using Speed 500 rpm

The PMSM running with reference speed set at 500 rpm and inverse speed (±500rpm). The speed response is shown in Figure 4.1. The quadrature and direct current (i_q, i_d) and three phase current (i_a, i_b, i_c) are shown in Figure 4.2 and Figure 4.3 respectively. From Figure 4.1 it shows that during initial condition it oscillates poorly. This is because no current and voltage involves during initial condition and it is hard for the estimator to calculate the speed.

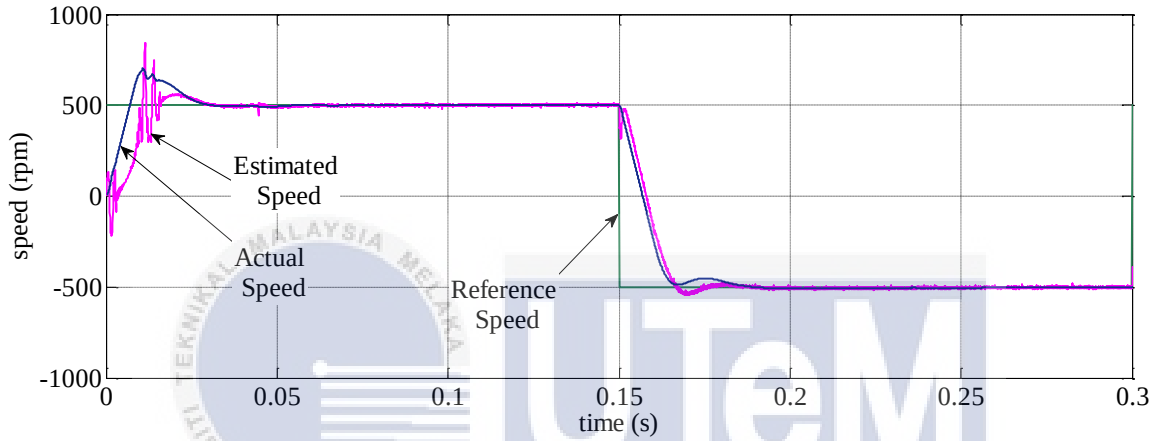

Figure 4.1: The speed response for 500rpm

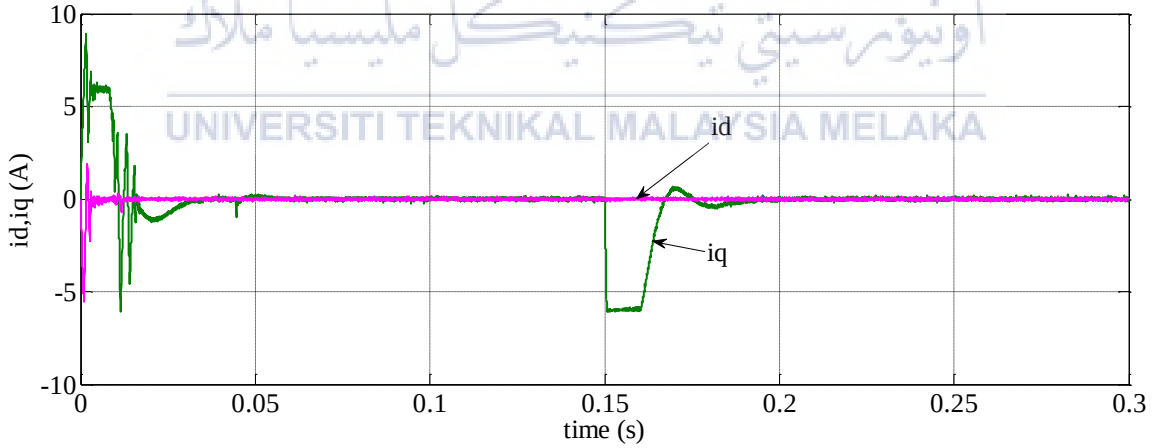

Figure 4.2: The quadrature and direct current response for 500 rpm

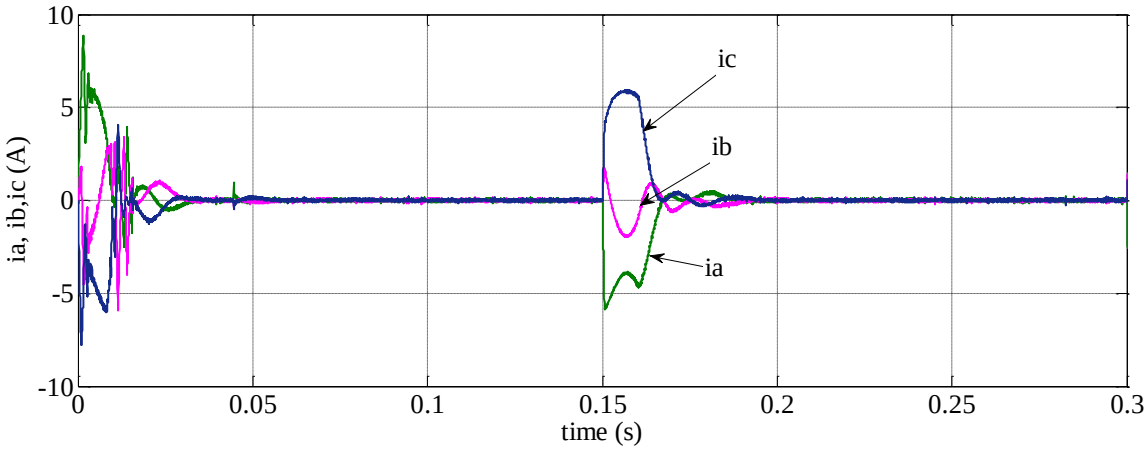

Figure 4.3: Three phase output current for 500rpm

The first simulation case shows the performance of the PMSM at 500rpm and inverse speed from 500rpm to -500rpm. Figure 4.1 to Figure 4.3 are the simulation regarding the speed response, quadrature and direct current response and the three phase output current. In Figure 4.1 it shows that the speed of motor has good dynamic response with a slight high overshoot. This proves that the system is able to operate at low speed of 500rpm.

4.2.2 Simulation Result using Speed 1000 rpm

The PMSM running with reference speed set at 1000 rpm and inverse speed ($\pm$1000rpm). The speed response is shown in Figure 4.4. The quadrature and direct current (i_q, i_d) and three phase current (i_a, i_b, i_c) are shown in Figure 4.5 and Figure 4.6 respectively. In Figure 4.4 it shows that the overshoot is less than 500rpm.

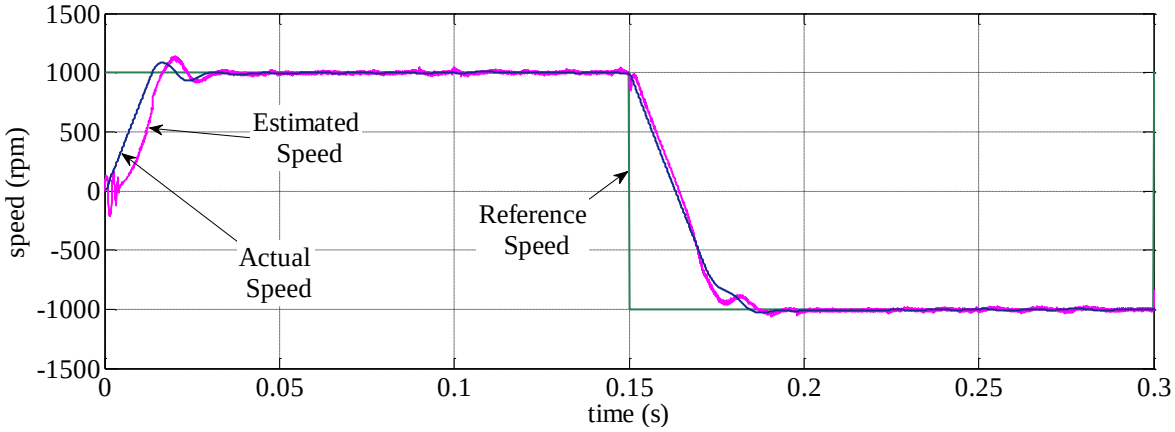

Figure 4.4: The speed response for 1000rpm

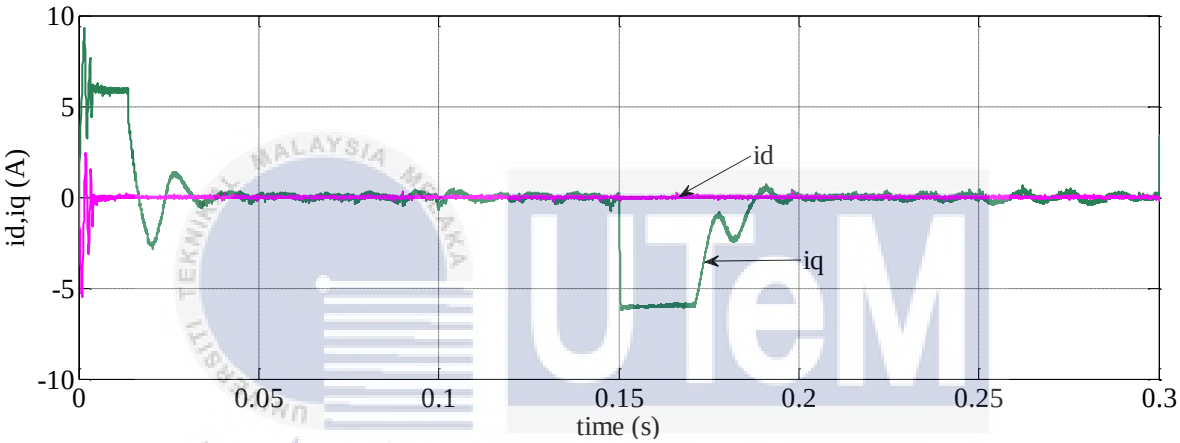

Figure 4.5: The quadrature and direct current response for 1000 rpm

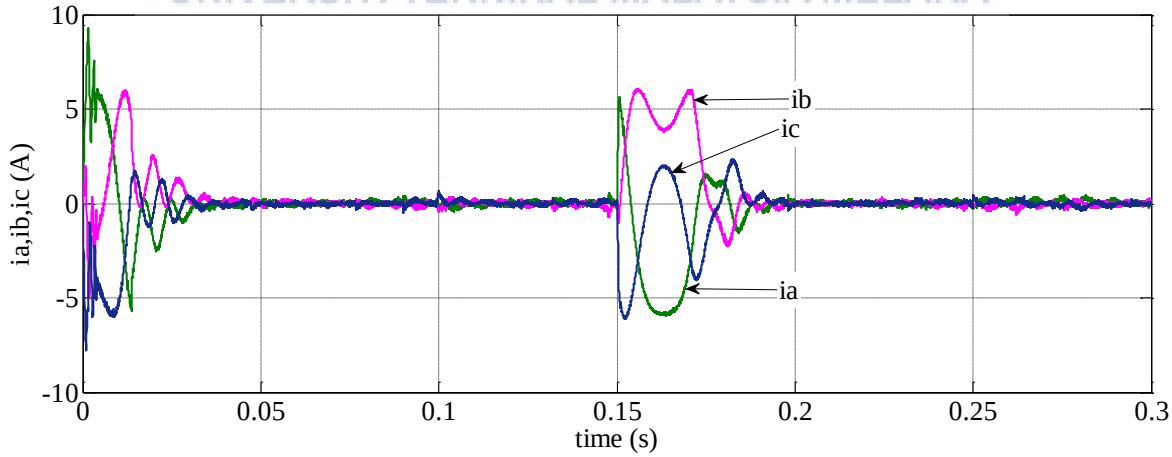

Figure 4.6: Three phase output current for 1000rpm

The Figure 4.4 to Figure 4.6 presents the PMSM running at speed of 1000rpm and inverse speed from 2000rpm to -2000rpm. The result shows that the estimated rotor speed can track well to the actual rotor speed and give good speed response. The overshoot for speed 1000rpm is less compared to speed of 500rpm. There are also changes in the three phases current as shown in Figure 4.6.

4.2.3 Simulation Result using Speed 1500rpm

The PMSM running with reference speed set at 1500 rpm and inverse speed ($\pm$1500rpm). The speed response is shown in Figure 4.7. The quadrature and direct current (i_q, i_d) and three phase current (i_a, i_b, i_c) are shown in Figure 4.8 and Figure 4.9 respectively.

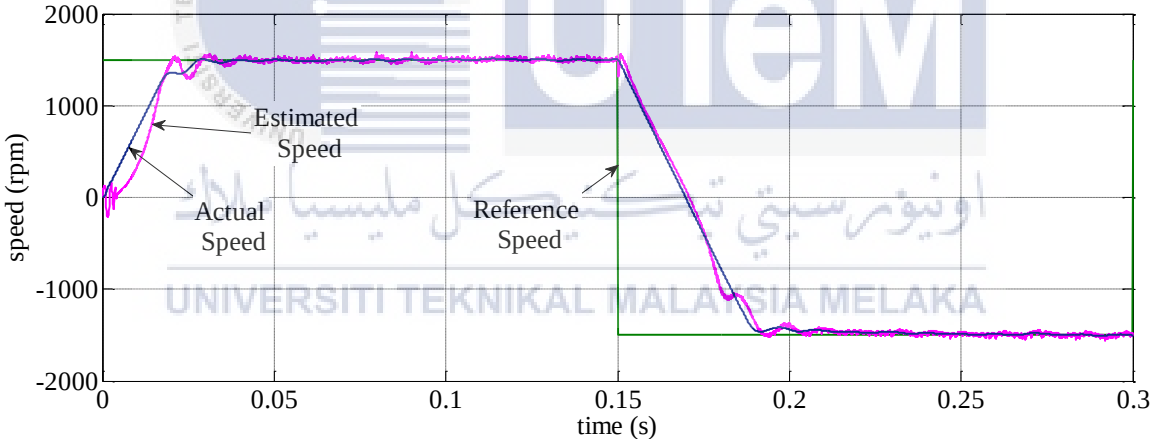

Figure 4.7: The speed response for 1500rpm

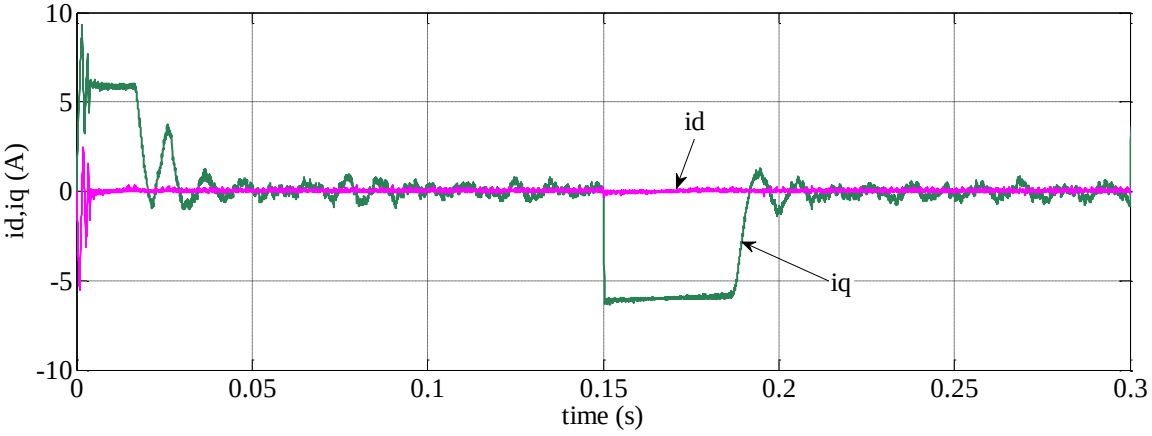

Figure 4.8: The quadrature and direct current response for 1500 rpm

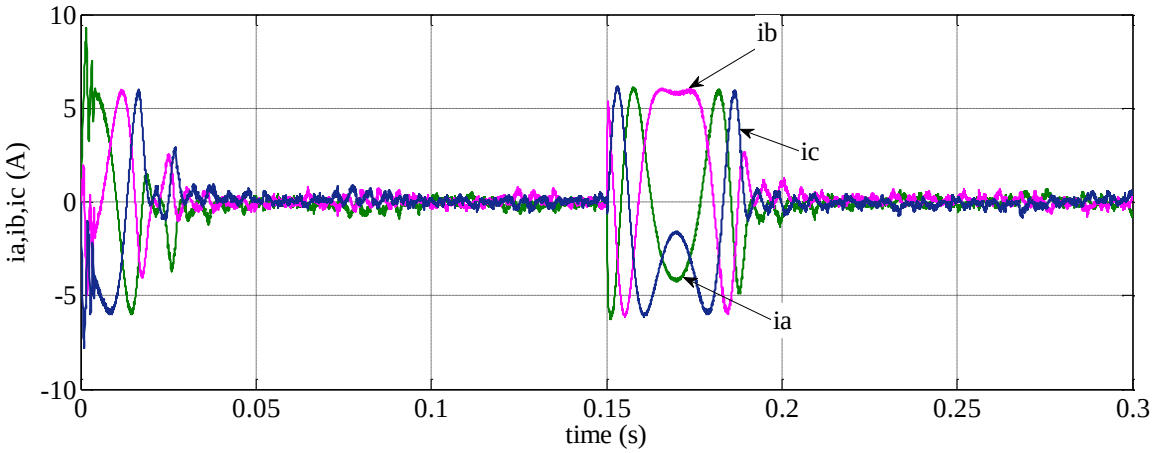

Figure 4.9: Three phase output current for 1500rpm

In Figure 4.7 to Figure 4.9, these figures represent the PMSM running at speed of 1500rpm and inverse speed from 3000rpm to -3000rpm. The result in Figure 4.7 shows that the output from estimator values can give a good follow to the actual rotor value. Other than that, the simulation result regarding the quadrature and direct current response shown in Figure 4.2, 4.2 and 4.8 indicate that the vector control is successful as i_d is controlled to zero.

4.2.4 Zoom View

i Forward Operation

Figure 4.10 presents the zoom view of the forward operation. The forward operation for speed of 500rpm, 1000rpm and 1500rpm are shown in Figure 4.10(a), 4.10(b) and 4.10(c) respectively. The simulation shows that, as the speed is increase the overshoot decrease for both actual and estimated speed. It shows that the estimated speed is able to follow the actual speed. However, the estimated speed response is not as good as the actual speed response. This reason is because during the initial condition, there are no current and voltage induced. This makes the response for estimated speed during initial condition inaccurate and oscillates.

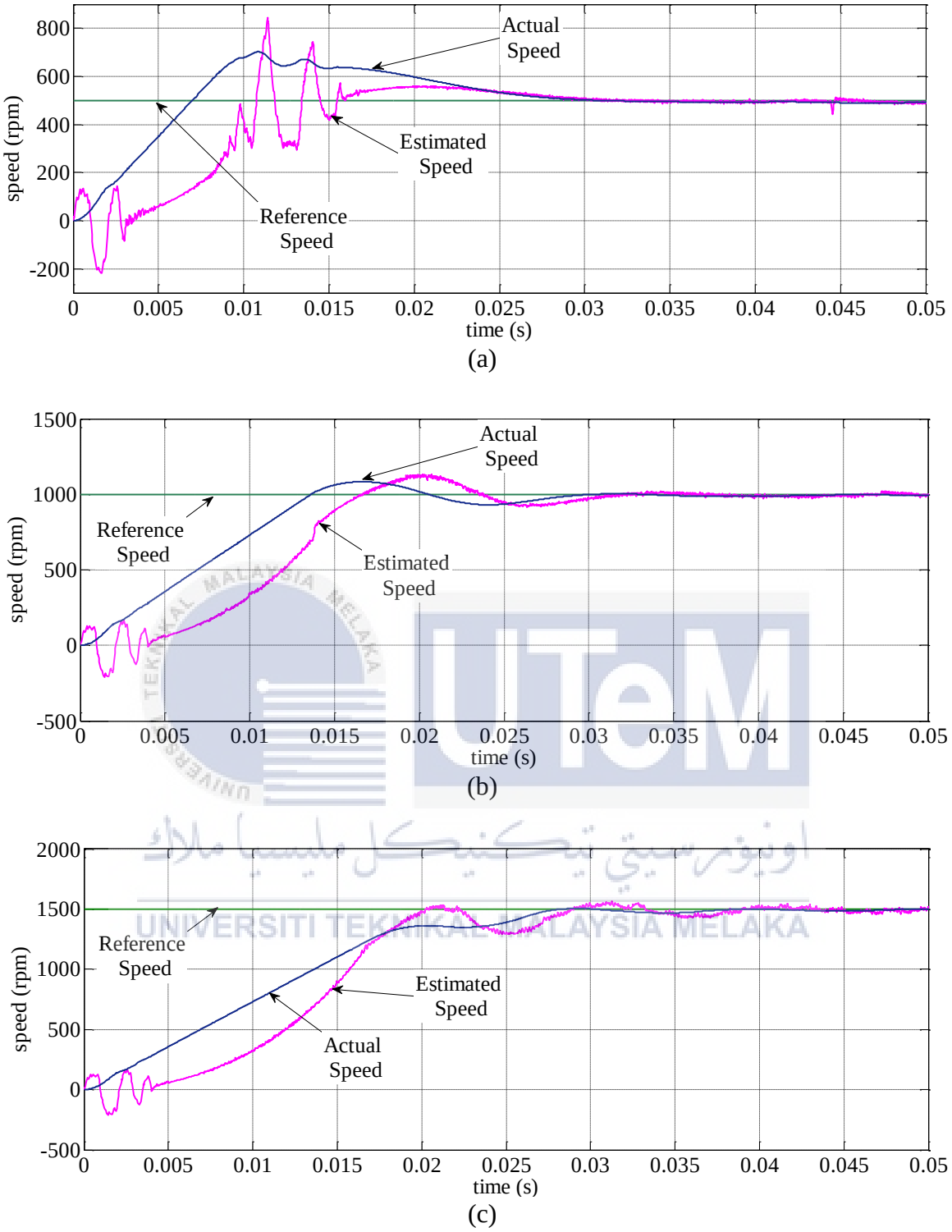

Figure 4.10: Zoom view simulation results for forward operation at speed of (a) 500rpm, (b) 1000rpm, (c) 1500rpm

ii Reverse Operation

Figure 4.11 presents the zoom view of the reverse operation. The reverse operation for speed of 500rpm, 1000rpm and 1500rpm are shown in Figure 4.11(a), 4.11(b) and 4.11(c) respectively. The system estimated speed can follow close to actual speed without huge overshoot.

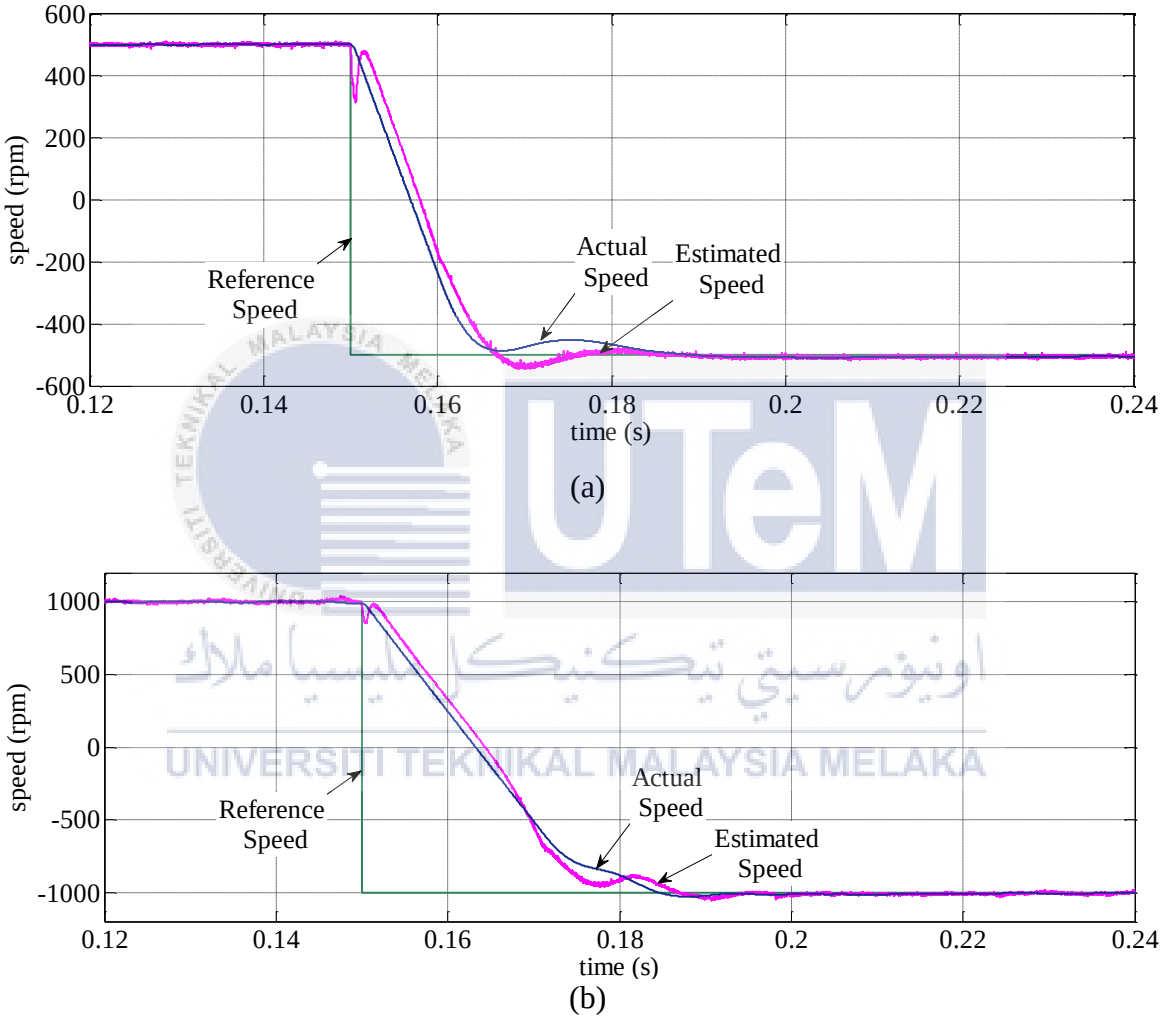

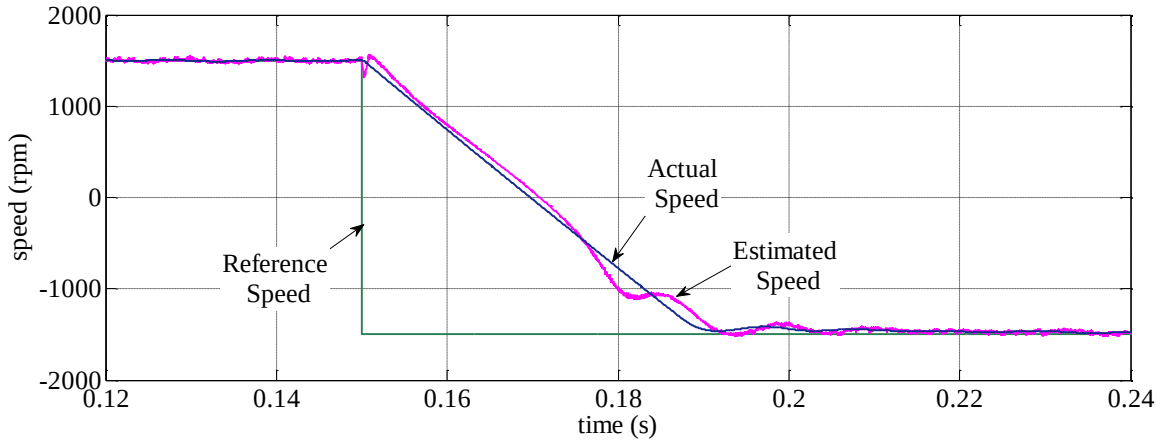

(c)

Figure 4.11: Zoom view simulation results for reverse operation at speed of (a) 500rpm, (b) 1000rpm, (c) 1500rpm

4.2.5 Loaded Condition

i. Operation at 1000rpm with load

The PMSM is tested with load of 4Nm at time 0.1s. Figure 4.12 below shows the (a) speed response, (b) The quadrature and direct current (i_q, i_d), (c) three phase current (i_a, i_b, i_c) respectively when load is applied. The undershoot drop is 156.6 rpm when 4Nm is applied to the PMSM.

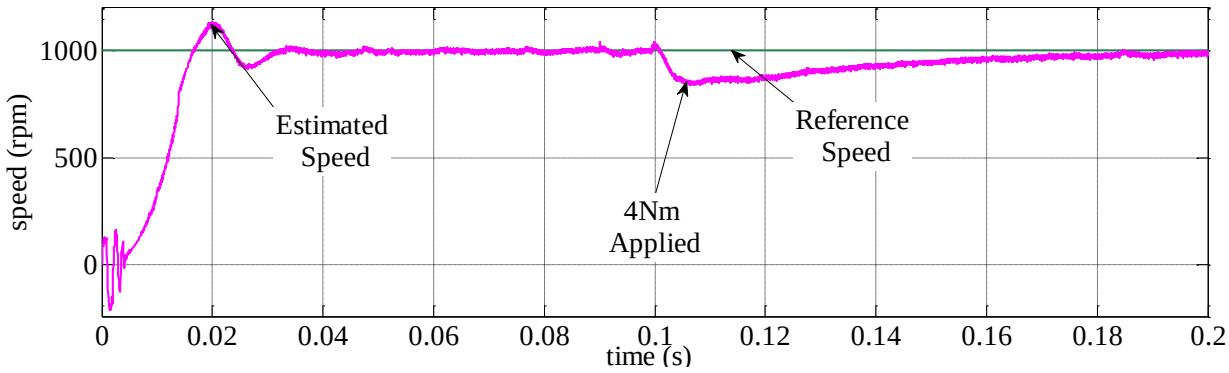

(a)

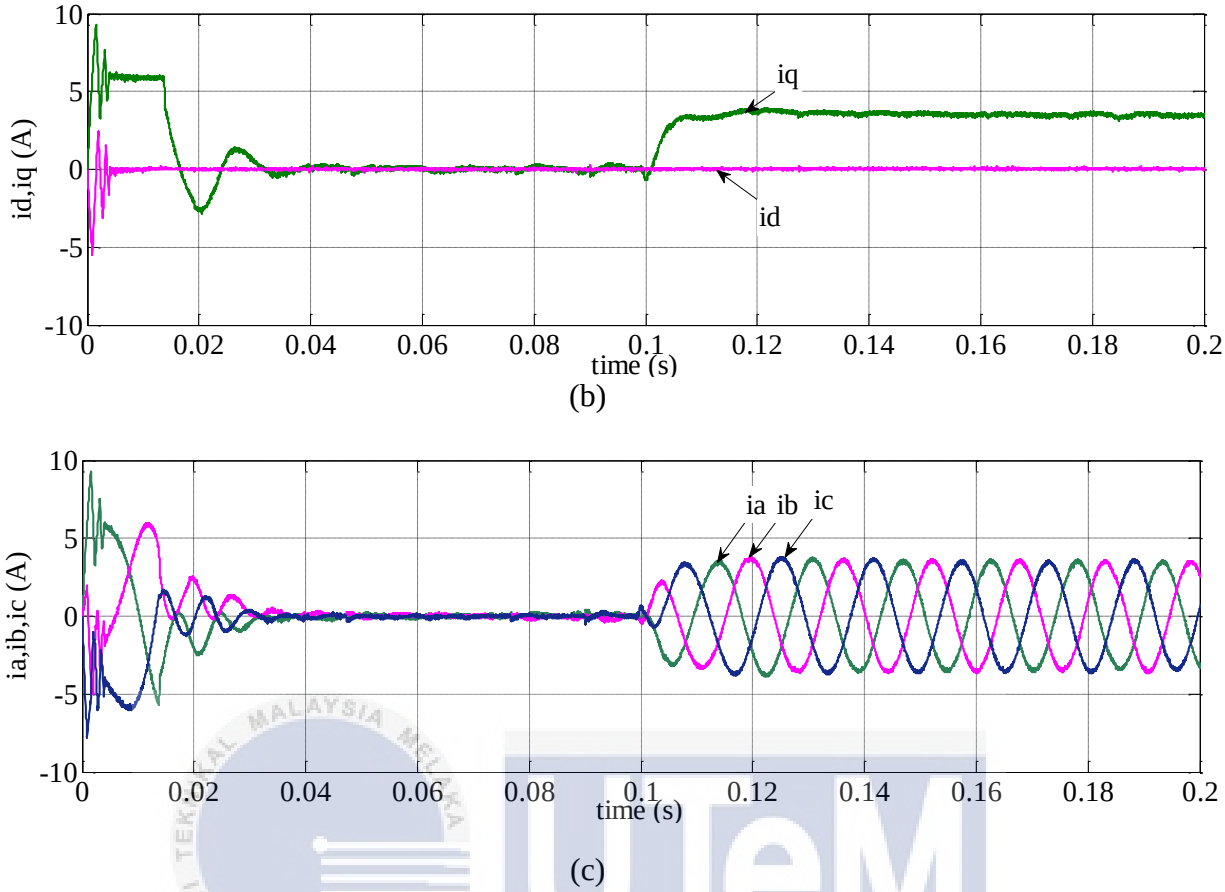

Figure 4.12: PMSM running at speed (1000rpm) with load of 4Nm (a) speed response, (b) quadrature and direct current and response (c)ia, ib and ic currents

Figure 4.12 below shows the speed response, the quadrature and direct current (i_q, i_d) and three phase current (i_a, i_b, i_c) respectively when load 4Nm is applied. The i_q is increase to 4.3A during load disturbance. This follows the i_q relationship as in equation 3.12.

ii. Load Variation

The PMSM is tested with applied load of 1Nm, 2Nm, 3Nm and 4Nm. Figure 4.13 below shows the undershoot simulation for (a) speed response 500rpm, (b) speed response 1000rpm (c) speed response 1500rpm. The undershoot drop increase directly proportional to the increase of load.

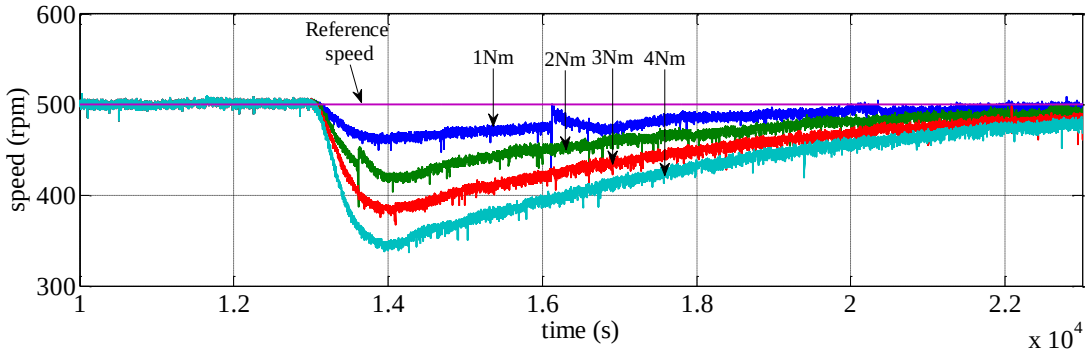

Figure 4.13 (a): The load variation at speed 500rpm for estimated speed

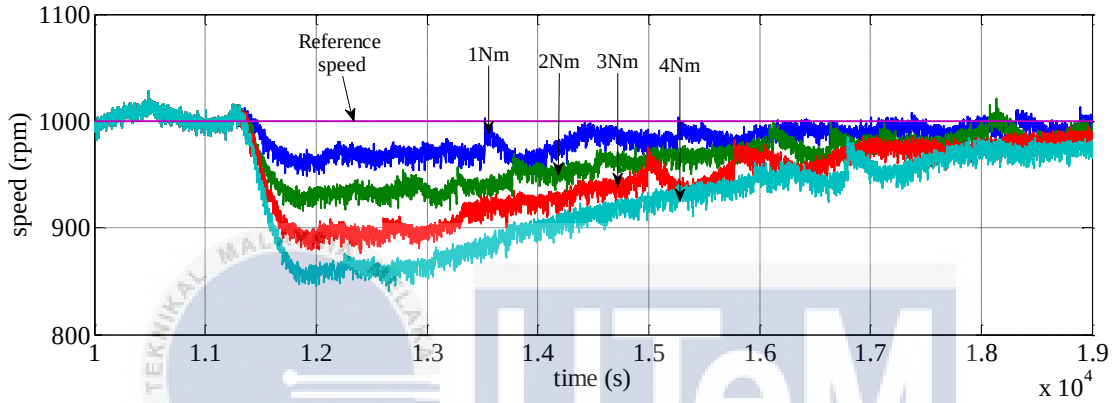

Figure 4.13(b): The load variation at speed 1000rpm for estimated speed

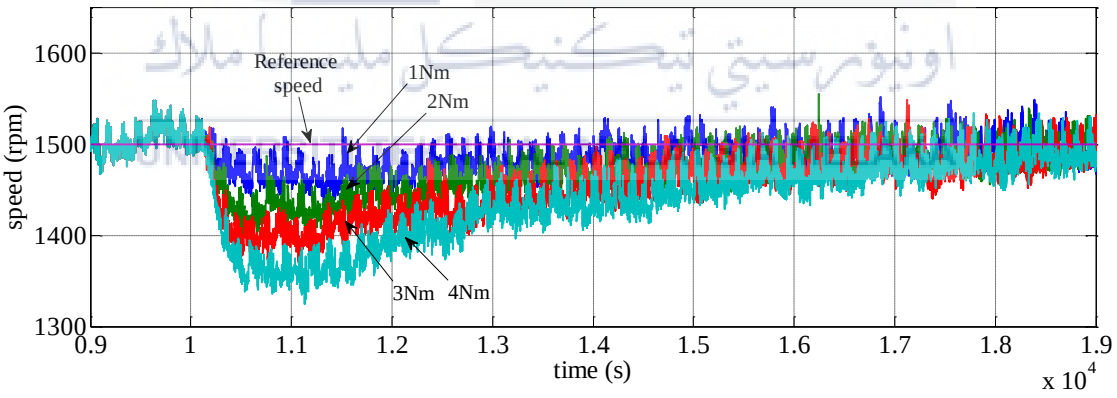

Figure 4.13(c): The load variation at speed 1500rpm for estimated speed

4.3 Summary of Result

The summary results for the speed of 500rpm, 1000rpm and 1500rpm is shown in the table below. Each of the table is separated for rise time, overshoot and undershoot with load disturbance. Table 4.1 shows the rise time trend for each speed of 500rpm, 1000rpm and 1500rpm. The graph in Figure 4.14 indicates that the estimated speed have faster rise time than actual PMSM drive speed. These show that the estimator rotor speed can follow well the actual rotor speed.

Table 4.1: Rise time for various speeds

Speed (rpm)	Rise Time (ms)	
	Estimated	Actual
500	5.231	9.594
1000	13.434	14.723
1500	15.95	16.338

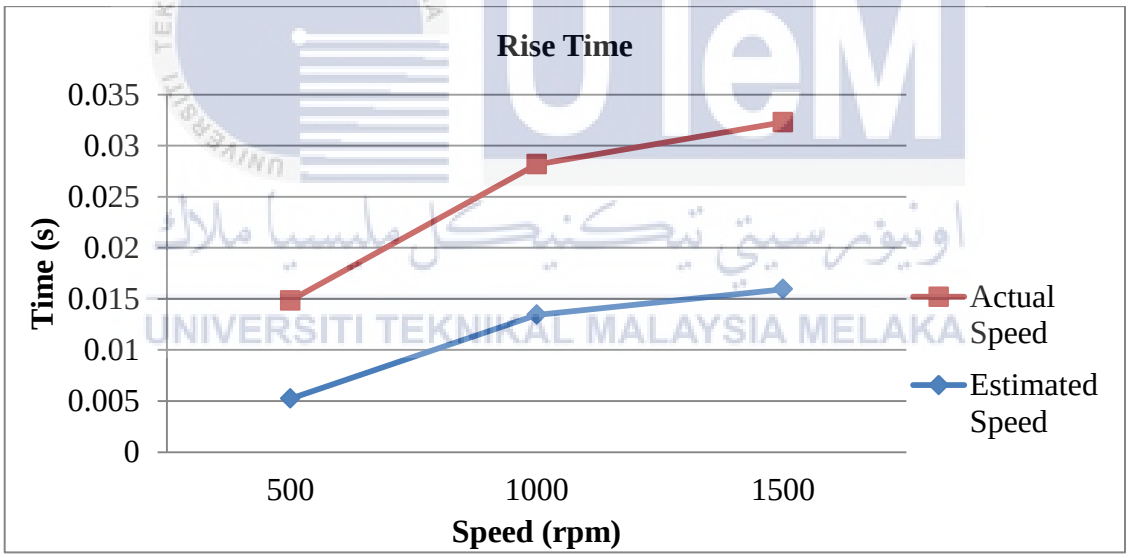

Figure 4.14: The rise time graph for speed of 500rpm, 100rpm and 1500rpm

Next for overshoot, the results are shown in Table 4.2. Based on the graph in Figure 4.15 it shows that speed from estimator has a slight higher overshoot than actual speed. The estimated response is able to follow the actual speed but it is not as good as the actual speed. This happens because during the initial condition, the value of voltage and current used in the estimator are not as accurate as steady state condition. This leads the response for estimated speed during initial condition to be inaccurate and oscillates.

Table 4.2: Overshoot for various speeds

Speed (rpm)	Overshoot (rpm)	
	Estimated	Actual
500	343.5	202.5
1000	132	83
1500	85	13

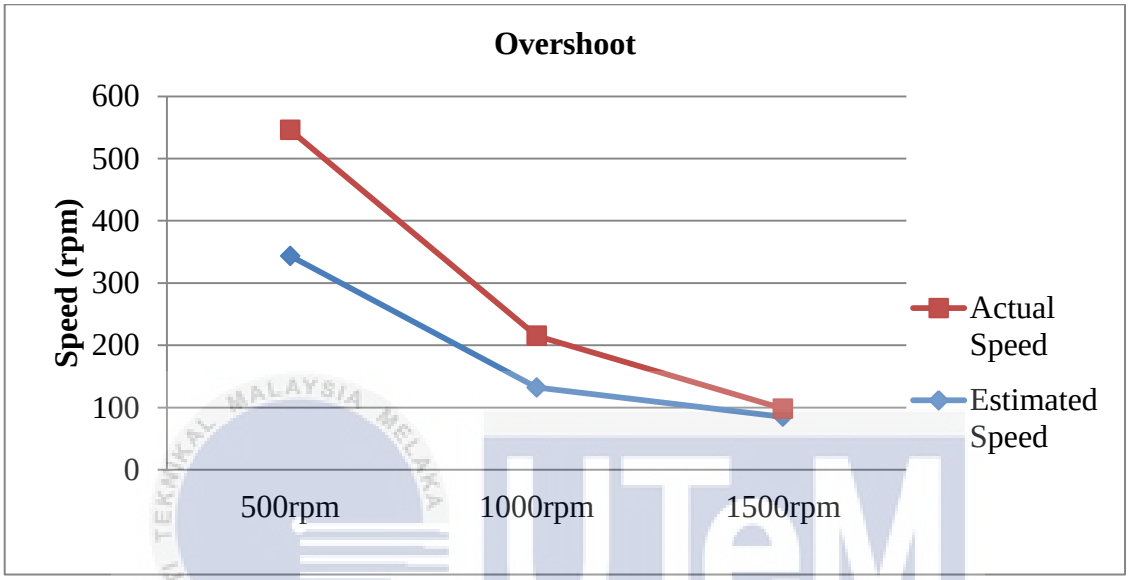

Figure 4.15: The overshoot graph for speed of 500rpm, 100rpm and 1500rpm

Furthermore, for Table 4.3 is the summarization of the undershoot values when different load of 1Nm, 2Nm, 3Nm, 4Nm is applied to the PMSM drive for speeds of 500rpm, 1000rpm and 1500rpm. From Figure 4.16, it can be concluded that the undershoot value increases with the increase of applied load to the PMSM system.

Table 4.3: Undershoot for various speeds with load variation

Speed (rpm)	Load Disturbance (Undershoot, rpm)			
	1Nm	2Nm	3Nm	4Nm
500	34.3	79.9	112.6	151.1
1000	38	64.1	104.1	150
1500	53	72	101	155

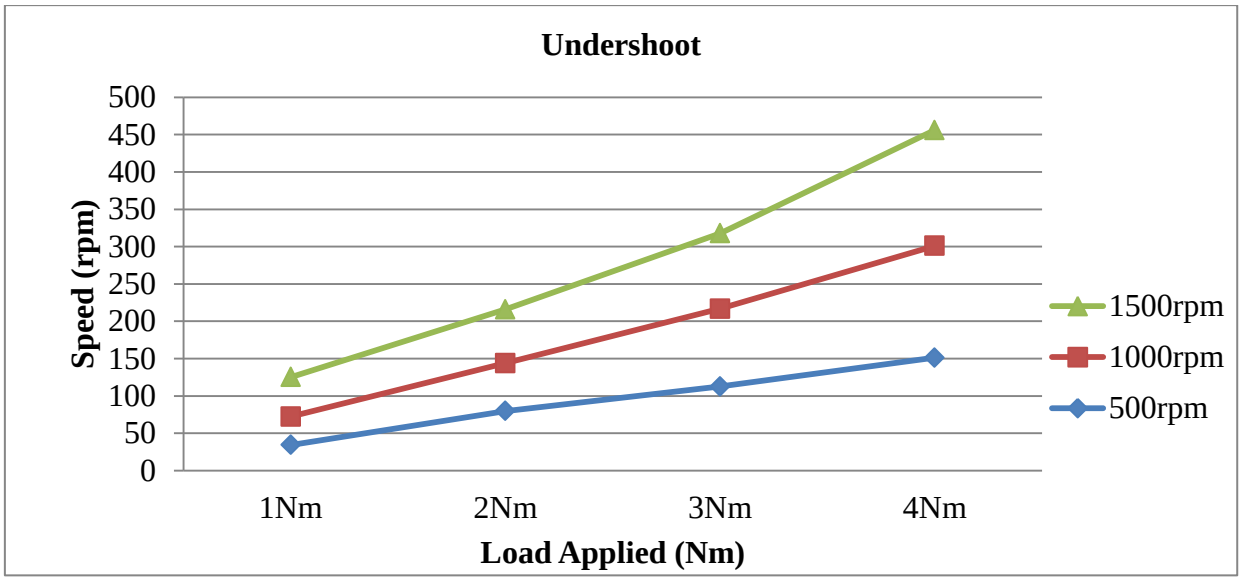

Figure 4.16: The undershoot graph for various speed when load applied

Therefore, based on the Figure 4.14 and Figure 4.15. The rise time and overshoot shows that the estimated results value is near to the actual results. Therefore it is concluded that estimated rotor speed are able to give similar or close follow to the actual rotor speed. Thus it shows that sensorless system is comparable with system with sensor as well as reducing the cost and size of system.

CHAPTER 5

CONCLUSION AND RECOMMENDATION

5.1 Conclusion

This project presented a sensorless PMSM drive. The performance is demonstrated through simulation by using Simulink. The sensorless technique selected is speed and position estimator using adaptive controller. By using sensorless PMSM drive, it reduces the size, cost, maintenance and complexity of the drive.

The sensorless PMSM drive using speed and position estimator has been successfully modelled and simulated using MATLAB/Simulink program. The simulation has been given various operating. In this simulation, the PMSM drive is tested for load and no load condition using three different speeds such as 500rpm, 1000rpm and 1500rpm.

From the rise time result taken from the simulation, the estimator rotor speed rise time is faster compared to actual rotor speed. Whereas for the overshoot, speed from estimator have a slight higher overshoot than actual speed but the estimator is still able to provide good performance. This shows that the use of estimator in sensorless PMSM drive allows the estimated rotor speed to track well the actual rotor speed. Furthermore the

PMSM is tested with different load of 1Nm, 2Nm, 3Nm and 4Nm and it shows that the undershoot value is higher when applied load is increase. In conclusion, it is shown that a sensorless system can provide similar performance or response to a system that used sensor. Lastly, the objectives of this project which are to model, develop, simulate and investigate the behaviour of sensorless Permanent Magnet Synchronous Motor (PMSM) drives using Fundamental Excitation are achieved.

5.2 Recommendation

As the recommendation, experimental testing of the PMSM can be carried out. The experimental testing can be done by doing hardware implementation. It is to prove that the performance of the sensorless PMSM drives using simulation and experimental is the same.

REFERENCE

[1] Yoon-Seok Han; Jung-Soo Choi; Young-Seok Kim, "Sensorless PMSM drive with a sliding mode control based adaptive speed and stator resistance estimator," in Magnetics, IEEE Transactions on , vol.36, no.5, pp.3588-3591, Sep 2000.

[2] Ying-Shieh Kung; Nguyen Trung Hieu, "Simulink/Modelsim co-simulation of EKF-based sensorless PMSM drives," in Power Electronics and Drive Systems (PEDS), 2013 IEEE 10th International Conference on , vol., no., pp.709-713, 22-25 April 2013.

[3] Prasad, E., B. Suresh, and K. Raghuveer. "Field Oriented Control of PMSM Using SVPWM Technique." Global Journal of Advanced Engineering Technologies 1.2 (2012): 39-45.

[4] Ching-Tsai Pan; Yi-Shuo Huang; Tai-Lang Jong, "A constant hysteresis-band current controller with fixed switching frequency," in Industrial Electronics, 2002. ISIE 2002. Proceedings of the 2002 IEEE International Symposium on , vol.3, no., pp.1021-1024 vol.3, 2002

[5] P. Enjeti, P. D. Ziogas, L. F. Lindsay, and M. H. Rashid, “A novel current controlled PWM inverter for variable speed ac drives,” in IEEE/IAS 1986 Annu. Meet., pp. 235–243.

[6] Jena, Satyaranjan; Chitti Babu, B.; Samantaray, S.R.; Mohapatra, Mohamayee, "Comparative study between adaptive hysteresis and SVPWM current control for grid-connected inverter system," in Students' Technology Symposium (TechSym), 2011 IEEE , vol., no., pp.310-315, 14-16 Jan. 2011

[7] Ying-Shieh Kung; Nguyen Vu Quynh; Chung-Chun Huang; Liang-Chiao Huang, "Design and simulation of adaptive speed control for SMO-based sensorless PMSM

drive," in Intelligent and Advanced Systems (ICIAS), 2012 4th International Conference on , vol.1, no., pp.439-444, 12-14 June 2012

[8] Pillay, P.; Krishnan, R., "Modeling of permanent magnet motor drives," in Industrial Electronics, IEEE Transactions on , vol.35, no.4, pp.537-541, Nov 1988

[9] Pillay, P.; Krishnan, R., "Application characteristics of permanent magnet synchronous and brushless DC motors for servo drives," in Industry Applications, IEEE Transactions on , vol.27, no.5, pp.986-996, Sep/Oct 1991

[10] Perera, PD Chandana. Sensorless control of permanent-magnet synchronous motor drives. Diss. AALBORG UNIVERSITY AALBORG, 2002.

[11] R. Krishnan, Electric Motor Drives Modeling, Analysis, and Control Pearson Education, 2001.

[12] Bimal, K. "Bose." Modern power electronics and AC drives (2002).

[13] Retrieved on 28 November,2015 from

http://machinedesign.com/sensors/basics-rotary-encoders-overview-and-new-technologies-0

[14] Gustavsson, Martin, and Viktor Frimodig. "Virtual Prototyping and Physical Validation of an Inverted Pendulum:" Sea-Calf Bot"." (2015).

[15] Gieras, Jacek F. Permanent magnet motor technology: design and applications. CRC press, 2002.

[16] Sul, Seung-Ki. Control of electric machine drive systems. Vol. 88. John Wiley & Sons, 2011.

[17] Prasad, E., B. Suresh, and K. Raghuveer. "Field Oriented Control of PMSM Using SVPWM Technique." Global Journal of Advanced Engineering Technologies 1.2 (2012): 39-45.

[18] Dorin O.Neacsu. SPACE VECTOR MODULATION- An Introduction, IECON'01: The 27th Annual Conference of the IEEE Industrial Electronic Society, 2001, pp.1583-1584.

[19] Wang, Wenjie, Zexiang Li, and Xiang Xu. "A novel smooth transition strategy for BEMF-based sensorless drive startup of PMSM." Intelligent Control and Automation (WCICA), 2014 11th World Congress on. IEEE, 2014.

[20] Kung, Ying-Shieh, and Nguyen Trung Hieu. "Simulink/Modelsim Co-simulation of EKF-based Sensorless PMSM drives." Power Electronics and Drive Systems (PEDS), 2013 IEEE 10th International Conference on. IEEE, 2013.

[21] Chi, Song. Position-sensorless control of permanent magnet synchronous machines over wide speed range. Diss. The Ohio State University, 2007.

[22] Urbanski, Konrad. "Sensorless control of PMSM high dynamic drive at low speed range." Industrial Electronics (ISIE), 2011 IEEE International Symposium on. IEEE, 2011.

[23] Han, Yoon-Seok, Jung-Soo Choi, and Young-Seok Kim. "Sensorless PMSM drive with a sliding mode control based adaptive speed and stator resistance estimator." IEEE Transactions on magnetics 36.5 (2000): 3588-3591.

[24] Carpaneto, M., M. Marchesoni, and G. Parodi. "A sensorless PMSM drive operating in the field weakening region using only one current sensor." 2010 IEEE International Symposium on Industrial Electronics. 2010.

[25] Pillay, Pragasen, and Ramu Krishnan. "Modeling, simulation, and analysis of permanent-magnet motor drives. I. The permanent-magnet synchronous motor drive." Industry Applications, IEEE Transactions on 25.2 (1989): 265-273.

[26] Xu, Kangping, et al. "Vector Control for PMSM." Sensors & Transducers (1726-5479) 170.5 (2014).

[27] Jung, J. I. N. W. O. O., and P. H. DStudent. "Project# 2 Space Vector PWM Inverter." 2005, The Ohio State University (2005).

[28] Arroyo, Enrique L. Carrillo. Modeling and simulation of permanent magnet synchronous motor drive system. Diss. University Of Puerto Rico Mayagüez Campus, 2006

[29] J. M. Lazi, Z. Ibrahim, SitiNoormiza Mat Isa, A. Anugerah, F. A. Patakor and R. Mustafa, "Sensorless speed control of PMSM drives using dSPACE DS1103

board," *Power and Energy (PECon), 2012 IEEE International Conference on*, Kota Kinabalu, 2012, pp. 922-927.

APPENDICES